Università degli Studi di Milano

Department of Biomedical Sciences for Health

PhD in Integrated Biomedical Research

XXX Ciclo

PhD Thesis

Stereophotogrammetric analysis of the human face:

a tool for modern morphologists

PhD Thesis by:

Valentina PUCCIARELLI

R10865

Advisor: Chiar. ma Prof.ssa Chiarella Sforza

ANNO ACCADEMICO 2016/2017

A mamma e papà

CONTENTS

ACKNOWLEDGEMENTS

At the end of my PhD program, I would like to express all my gratitude to my supervisor Professor Chiarella Sforza: you have been source of inspiration for me, both from a scientific point of view and for life. Thank you for everything I've learnt from you, both from the Professor and the Woman.

My gratitude goes also to Professor Claudia Dolci. Thank you for co-advising and helping me to become better day by day.

Many thanks to all the colleagues of the LAFAS and LAM laboratories: you have made this experience wonderful. I'm proud to have all of you as friends.

Last but not least, thank you to my parents: nothing would have been possible without your support and your love.

ABSTRACT

The introduction of new technologies has provided, in the last years, a significant contribution to anthropometry. In this context, facial anthropometry has greatly benefited from optical instruments such as laser scanners and stereophotogrammetry.

The latter technique has proven to be accurate, repeatable and fast; therefore, taking into consideration its non-invasive nature, it has been increasingly applied to medicine, due to the relevant support that anthropometry can provide to this field.

A facial anthropometric assessment can provide reliable morphometric details about the presence of deformities and peculiar features connected to underlying pathological conditions, not always easily recognizable. In the case of certain neurologic diseases, it can also provide new insights about the genotype/phenotype correlation taking the close relationship between facial and cerebral development into consideration.

Furthermore, the three-dimensional morphometric evaluation of the face can reveal objective parameters useful for the planning and assessment of maxillo-facial and dental treatments, thus facilitating the clinical decisions and increasing the patients' compliance.

The facial morphometric evaluations presented in the current thesis were performed through the VECTRA M3 3D stereophotogrammetric system (Canfield Scientific, Fairfield, NJ, USA). All the patients and control subjects involved were marked with a set of facial landmarks (adapted according to the different study purposes), before the acquisitions. Once the three-dimensional models were obtained, they were elaborated through the software of the stereophotogrammetric system. Data were analysed through different statistical techniques, according to the type of study executed. The morphometric evaluations were divided in two groups: facial morphometric analyses performed through a landmark-based approach and through a surface- based approach.

The first group included the studies: 1) "The face of adult patients affected by Dravet Syndrome: a 3D stereophotogrammetric preliminary assessment", 2) "3D Craniofacial morphometric analysis of GLUT-1 DS patients" and 3) "Stereophotogrammetric analysis of a case of holoprosencephaly".

The second group included the studies: 4) "3D stereophotogrammetric assessment of labial symmetry in a girl treated for a lymphatic malformation" and 5) "Facial reanimation assessment performed through 3D-3D superimposition: a new method".

For both assessed syndromes, study 1 and 2 allowed the individuation of facial features common among the patients, whose recognition can have a role in the diagnosis of the disease, both in children (study 2) and in adult cases (study 1). Study 3 allowed the identification of the presence of dysmorphic facial features in a girl affected by holoprosencephaly with an apparently normal aspect, thus sustaining the potential of the 3D stereophotogrammetric facial analysis in the morphometric characterisation of the face. Study 4 and 5 showed the usefulness of this technique for performing an objective surgical follow-up and final evaluation of maxillo-facial treatments, helping clinicians in their decisions and motivating the patients.

In conclusion, all the studies sustained the usefulness, for medical purposes, of an anthropometric assessment of the human face, performed through a three-dimensional stereophotogrammetric analysis. Moreover, they highlighted its applicability to different categories of patients, including children and people with intellectual disability; thus again justifying the increasing diffusion of stereophotogrammetry in clinical and research centres.

Key words: anthropometry, stereophotogrammetry, face.

1. INTRODUCTION

Among the different districts that constitute our body the face has a main role. It contains the sensory organs and allows to communicate and interact with the external world; it is unique for anyone, also in the case of monozygotic twins, and permits personal identification. From this point of view, facial integrity has a great importance, both for functionality and for social life [1].

Furthermore, particular facial features can be associated with pathological conditions and their recognition offers the possibility of identifying them in an easy and early way. In this context, an example is represented by Down Syndrome, a genetic condition that shows a unique facial appearance, often associated with mental retardation [2,3].

The first method used to analyse and identify the characteristics of the face, which can also be applied to the rest of the human body, is represented by anthroposcopy. Being still applied in medicine, this technique consists of the mere observation of the facial features, qualitatively appreciated by an expert operator (e.g. clinician, morphologist), which relies on his/her internalised judgment criteria, developed during the course of a long-time experience [4].

Nevertheless, the possibility of directly measuring the face has permitted the development of anthropometry, which consists of a quantitative assessment of the facial features, aimed at providing objective measurements of their shape and size variations [5].

Both anthroposcopy and anthropometry have provided support to the medical practice, but the objectiveness obtained from the anthropometric approach has produced a greater contribution to the medical field. In particular, it supports the diagnosis of the syndromes that present a facial involvement, the evaluation of the outcome of maxillo-facial and dental treatments and the assessment of normal and abnormal growth patterns [6-9].

Furthermore, anthropometry can be useful even when isolated cases of a particular condition are present, helping to integrate their clinical diagnosis and to classify them among better known conditions [4].

Nevertheless, with the technology advancement, anthropometry evolved. The use of simple measurement instruments such as callipers and measuring tapes, originally used to take direct measurements on subjects and patients, has been overcome by different measurement methods and currently different three-dimensional (3D) image analysers are available.

1.1 Three-dimensional image analysers

Three-dimensional image analysers can be classified into contact and non-contact instruments. The first category includes electromagnetic and electromechanical digitizers and ultrasound probes, while the second one consists of Magnetic Resonance Imaging (MRI), Computed Tomography (CT), optoelectronic instruments, laser scanners and stereophotogrammetry.

Contact instruments

Contact instruments need a direct contact with the acquired object (or face) to reconstruct it. They are made of a 3D digitising device that is used to measure and collect data, directly transmissible from the physical object into a connected computer. They are easy to use and portable, nevertheless this approach only allows the collection of the 3D coordinates of the landmarks identified by the 3D digitizing device [10,11].

Among them, the electromagnetic digitisers use a 3D digitising device which works as a sensor, moving in a specific magnetic field and contacting the surface to be acquired. Coordinates of the landmarks identified by the sensor can be collected and used to perform anthropometric measurements [10,12] (Figure 1.1). On the other hand, electromechanical digitisers use a mechanical or electromechanical sensor, which rotates as an arm around the object to acquire (e.g. dental cast), thus allowing the collection of the 3D coordinates of the touched points [12, 13] (Figure 1.2).

Eventually, contact instruments include ultrasound probes. These instruments use acoustic waves (in the Megahertz frequency) to reconstruct, in real time, the 3D anatomy of the investigated anatomical structures (e.g. internal organs of a patient) without using ionizing radiations. For this reason, they are widely used in prenatal diagnosis, providing morphological information about the foetal health status [12,14].

Non-contact instruments

This category of instruments does not require the physical contact with the object/subject to be acquired. This is particularly relevant in the case of acquisition of soft tissues, as for facial morphometric analysis; indeed, the absence of tissue-instrument interaction reduces the possibility of contact artefacts and ensures a faster acquisition procedure. Among them, optical instruments such as laser scanners and stereophotogrammetric instruments have wide applications in the medical, forensic and technical fields [12]. In contrast, MRI and CT are

volumetric instruments that are mostly used for clinical purposes, even if their application in the morphometric field has been proposed [15].

Laser scanners use a laser light source which is reflected by the object/subject to be acquired, thus allowing the calculation of the time and, consequently, the distance between the light source and the acquired surface. They can be unmovable or portable and their accuracy and reliability in the 3D surface reconstruction have already been evaluated (Figure 1.3a,b) [16,17].

In the case of subject scans, as for facial reconstructions, it is requested that the subjects remain still for the whole procedure; the contactless technology facilitates this phase.

Table laser scanners have also been validated for the reconstruction of 3D inanimate objects. An example of table laser scanner is provided by the dental laser scanner "Dental Wings Series 3" (Dental Wings Inc., Montreal, Canada), widely used in our laboratory even if it will not be mentioned in the studies reported in this thesis (Figure 1.4) [18,19].

Eventually, stereophotogrammetric systems use couples of coordinated cameras to acquire facial images from different angulations. These images, captured in a fast time, are appropriately elaborated by a dedicated software, in order to obtain a 3D-surface reconstruction, coupled with a colorimetric texture. The use of visible light makes them non-invasive, thus allowing the execution of multiple acquisitions even in subjects that must not undergo facial imaging for medical reasons. The speed of acquisition permits the realisation of acquisitions in all kinds of subjects, including children and patients, even when they are not completely collaborative [20].

1.2 VECTRA M3 3D stereophotogrammetric system

The studies presented in this thesis have been performed using the stereophotogrammetric system VECTRA M3 3D (Canfield Scientific, Fairfield, NJ, USA). VECTRA M3 3D allows to simultaneously capture facial images in a 3.5 milliseconds time, obtaining 3D facial reconstructions with a geometric resolution of 1.2 mm.

The system is made up of 3 couples of coordinated cameras (1 black and white and 1 colour), sustained by 3 pods, each one including a light projector.

Visible light is projected on the face, in order to maximize the differences between facial areas and depth, then the images are simultaneously captured. A dedicated software (Mirror®) allows the 3D reconstruction and its subsequent manipulation. Calibration is required daily or anytime

the system is moved, in order to ensure accuracy and reliability of the acquisition procedure and the facial anthropometric data obtainable (Figure 1.5) [21].

Both laser scanners and stereophotogrammetric systems allow the obtainment of the reconstruction of the entire facial surface and are not limitated to some specific landmarks only [22].

From this point of view, in comparison to contact instruments, they allow the execution of both landmarks-based or surface-based facial morphometric analyses. For this reason, the studies presented in this thesis are based on both of these approaches or their combination.

1.3 Facial landmarks

Even if optical instruments allow the acquisition and reconstruction of the whole facial surface and are not dependent on the identification of specific landmarks to provide a 3D reconstruction; the direct identification of some facial reference points, before image acquisition, represents an important element that ensures a greater precision and accuracy of the subsequent measurements and allows a repeatable surface segmentation [12, 13, 23].

Differently from direct anthropometry, where landmarks identification allows the performance of direct instrumental measurements, digital anthropometry allows the collection of their 3D coordinates that can be used to calculate, through Euclidean geometry, different measurements, including linear distances and angles [12].

Landmarks identification must be performed by an expert operator because it can be affected by different error sources. While landmarks located on the skin surface are, indeed, easy to identify in healthy subjects, their localisation can be difficult in dysmorphic faces, where they can be missing or not properly localised. Furthermore, bony reference points can be easy to palpate if covered by a subtle fat layer, while their recognition can be problematic if the fat layer is thick [24].

1.4 Fifty landmarks protocol

Among all the classic facial anthropometric landmarks, in our laboratory a set of 50 was chosen to define a facial morphometric analysis protocol. This protocol was successively tested and, since its reliability, widely used. All the studies collected on this thesis, even those based on a surface approach, took advantage of it [25,26].

The protocol is composed of 3 phases:

- visual or palpatory landmark identification;
- landmark marking (performed with a biocompatible and washable black makeup eyeliner);

- landmark digitisation (performed on the reconstructed facial surface).

As mentioned above, in order to reduce the errors, the phase of landmarks identification directly on the skin of the subject facilitates their recognition in the digital reconstruction. Indeed, the palpatory nature of some of them makes their identification on the virtual reconstruction impossible or very prone to error [24].

According to this protocol the 50 landmarks are:

Trichion (**tr**): located in the midline, at the attachment of the hair;

Glabella (**g**): midline point, it is the most prominent point of the forehead;

Nasion (**n**): midline point, located at the suture between nasal and frontal bones;

Pronasale (**prn**): midline point, it is located at the tip of the nose;

Columella (**c**): midline point, located at the inferior limit of the nostrils;

Subnasale (**sn**): midline point, located at lowest point of the columella;

Labiale superius (**ls**): midline point, located between the upper vermillion border and the skin;

Stomion (**sto**): midline point, located in the middle of the lips;

Labiale inferius (**li**) midline point, located between the lower vermillion border and the skin

Sublabiale (**sl**):midline point, located in the mentolabial fold;

Pogonion (**pg**): midline point; it is the most prominent point of the chin;

Gnation (**gn**): midline point; located in the lower border of the mandibular body.

Paired landmarks, located in both facial halvers are:

Tragion (**t**):located at the level of the tragus;

Preaurale (**pra**): most anterior point of the ear margin;

Superaurale (**sa**): upper point of the ear margin;

Postaurale (**pa**): most posterior point of the ear margin;

Subaurale (**sba**); lower point of the ear margin;

Frontotemporale (**ft**): located on the forehead at the elevation of the temporal line;

Zygion (**zy**): most prominent point of the zygomatic arch;

Gonion (**go**): located at the mandibular angle;

Orbitale superius (**os**):located at the superior orbitary margin, at the level of the supraorbital notch

Orbitale inferius (**or**); lower point of the inferior orbitary arch;

Exocanthion (**ex**): extern ocular commissure;

Endocanthion (**en**): intern ocular commissure;

Cheek (**chk**): at the intersection between the lines “t-ac” and “ex-ch”;

Alar (**al**): most lateral point on the ala of the nose;

Alar crest (**ac**):most lateral point at the root of the nasal ala;

Inferior terminal of the nostril (**itn**): lower point of the nostril;

Superior terminal of the nostril (**stn**): upper point of the nostril;

Cheilion (**ch**): commessure of the mouth;

Crista philtri (**cph**): located at the elevated margin of the labial philtrum.

A complete series of 50 landmarks, individuated in a subject’s face is depicted in figure 1.6.
Different subsets of these points, adapted to the study object, were chosen for the different studies presented in this thesis. They were generally indicated through their acronym, followed, in the case of paired landmarks, by the letters l or r to specify their actual position.

1.5 Aim

The aim of this thesis is to present some examples of stereophotogrammetric facial morphometric analysis, in order to show its important application to the medical field.
Many genetic syndromes are, indeed, characterised by particular features that permit their identification among different conditions; nevertheless their clinical diagnosis can be, sometimes, troubling due to various problems [27,28]. Since the presence on the face of pathological gestalt signs, facial morphometric analysis can facilitate their recognition, sustaining (but not replacing) the clinical diagnosis.
The face has indeed a complex embryological development and many defects happened during embryonic life can alter its morphology. Moreover, other genetic insults can reflect themselves in facial development and appearance [29]. The non-invasive nature of the stereophotogrammetric systems makes them ideal tools to easily investigate facial morphology and to identify these “soft markers” of disease [20].
Reinforcing qualitative clinical experience with quantitative data, stereophotogrammetric analysis can also permit the execution of comparisons among individuals: related subjects, controls or patients [30,31]. Moreover, the possibility of three-dimensionally quantifying facial features can provide help in the planning, follow-up and outcome evaluation of surgical treatments (in maxillo-facial, dental, plastic and reconstructive surgical fields), thus supporting clinical practice and helping the patients to be confident and compliant to the treatment [7].

Figure 1.1. Electromagnetic digitizer [31].

Figure 1.2. Electromechanical digitizer [31].

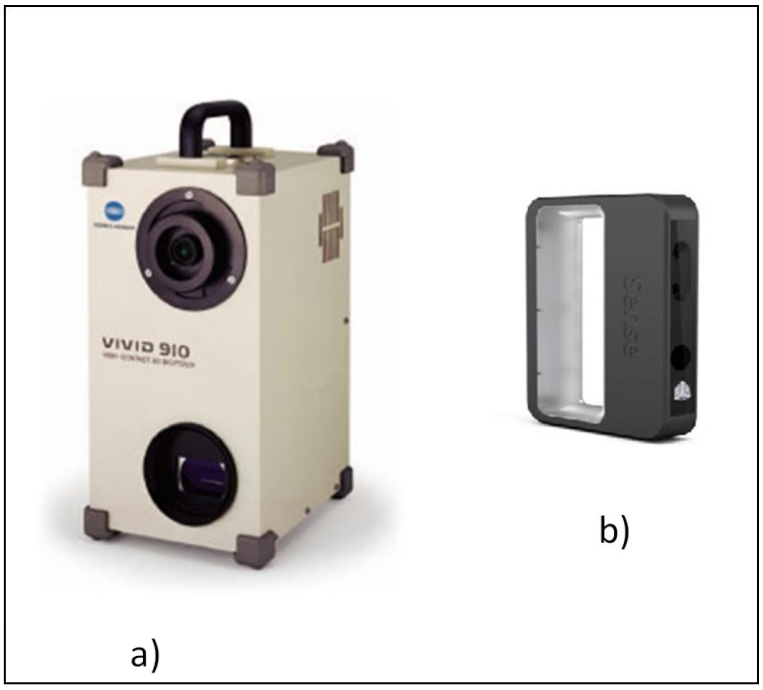

Figure 1.3. a) unmovable laser scanner; b) portable laser scanner.

(https://www.konicaminolta.eu/; https://www.3dsystems.com/shop/sense, accessed on August 25th 2017).

Figure 1.4. Dental laser scanner Dental wings series 3 (Dental Wings Inc., Montreal, Canada).

(http://www.dentalwings.com/it/prodotti/sistemi-di-scansione-e-modellazione/3series/ , accessed on August 25th 2017).

Figure 1.5. VECTRA M3 3D (Canfield Scientific, Fairfield, NJ, USA).

(http://www.canfieldsci.com/, accessed on August 25th 2017).

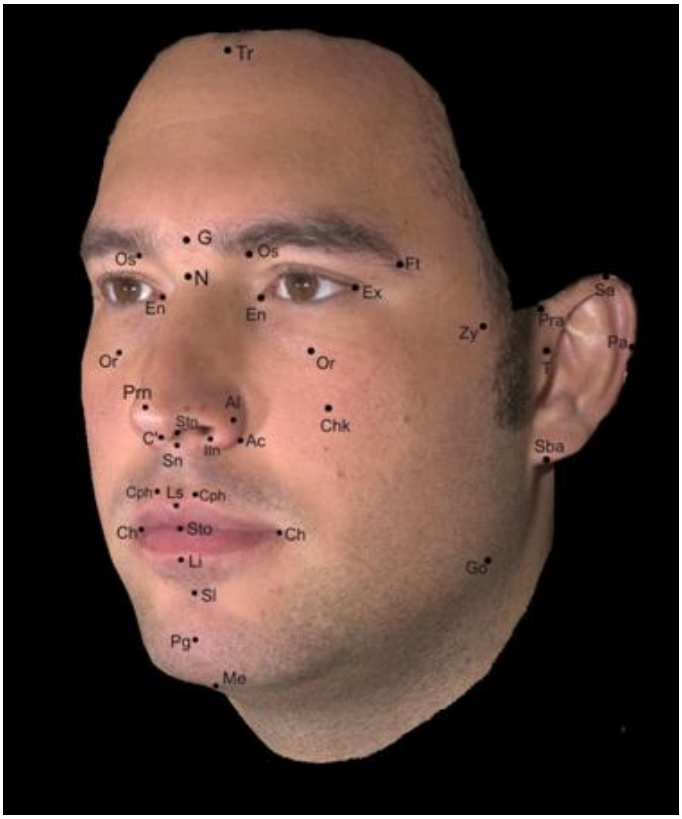

Figure 1.6. Soft tissue facial landmarks digitized on all subjects [31].

2. FACIAL MORPHOMETRIC ANALYSIS: LANDMARKS-BASED APPROACH

In this section will be reported some studies, executed by mean of a stereophotogrammetric analysis of the face and conducted through a landmark-based approach, according to the protocol defined in paragraph 1.4.

As previously mentioned, stereophotogrammetry allows the reconstruction of the entire facial surface, thus permitting to virtually obtain the coordinates of all the landmarks that constitute the surface. Nevertheless the x, y and z coordinates of some points of interest, previously marked, can be extracted and used to perform anthropometric calculations or more complex analyses [12,32].

2.1 Study 1: The face of adult patients affected by Dravet Syndrome: a 3D stereophotogrammetric preliminary assessment.

Initially indicated as “Severe Myoclonic Epilepsy of the Infancy” (SMEI) and then renamed “Dravet Syndrome” (DS), from the name of the French scientist who described it for the first time, DS (OMIM #607208) is an early onset epileptic encephalopathy, arising in association with fever episodes during the first year of life of apparently healthy children [33,34]

The syndrome has a genetic origin, being linked to more than 500 mutations of the gene SCNA1, which encodes for the subunit α1 of the voltage-dependent sodium channel (Nav 1.1) [35]; 40% of the mutations are truncating, being the remaining missense and splice site. Ninety-five per cent of them occur *de novo*, thus explaining the unaffected status of the different members of the same family. Nevertheless, some familiar cases were described in literature [36-38].

For what concerns the clinical features, the syndrome begins in apparently healthy children, and it is characterized by generalized or unilateral clonic seizures, exacerbated by fever. Mental decline and movement disorders including ataxia, may complete the clinical picture [33,39].

The phenotype of the disease is progressive and, with time, seizures may become myoclonic, partial or absence. A psychomotor stagnation is also present, generally starting from the second year of age, together with an evolution of pyramidal signs and ataxia; personality disorders may occur and are generally of varying intensity [40].

With time, the progressive cognitive decline, present at various levels in DS patients, also involves the linguistic skills, with a certain maintenance of the language comprehension and a reduction of the productive abilities, at least for the first years from the disease‘s beginning [41-44].

Electroencephalography, which is often normal at the disease onset, may show signs of anomalies during disease evolution in absence of a precise pattern, although brain imaging results are generally normal [45].

In consideration of the diffuse resistance of DS to the therapy and the fact that the consumption of sodium channel blockers can also exacerbate a status epilepticus, the treatment of this condition must be adapted to each patient and, generally, involves a combination of different antiepileptic drugs. Surgery, like callosotomy and vagal nerve stimulation, has also been attempted and the introduction of ketogenic diet has been investigated in animal models and in humans [46-48].

Since the typical clinical early presentation of the syndrome co-exists with a wide phenotypical variability including, for example, a history of chronic migraine at the mildest end of the spectrum, many adult cases remain undiagnosed [49].

The aim of this preliminary study is to analyse the three-dimensional facial morphology of a group of DS patients in order to verify, among them, the presence of typical facial features that can be useful for the identification of the disease in undiagnosed adults and in cases of peculiar disease presentation.

2.2 MATERIALS AND METHODS

The patients analysed included three females and three males of age comprised between 16 and 37 years that had received a clinical diagnosis of DS during infancy. The diagnosis had successively been confirmed by the mutational analysis of the SCN1A gene that revealed the presence of a missense mutation for 4 of them and the presence of a nonsense mutation for 2 of them.

Three hundred ninety-six control subjects, paired for age, sex and ethnicity were also analysed. Details about the patients analysed and paired control subjects are provided in table 2.1. None of them had facial deformities or surgical or traumatic outcomes.

All procedures, which were completely riskless, were executed following the tenets of the Declaration of Helsinki, after approval by the local ethic committee and after the signature of a written consent by the interested subject or his/her parents or legal guardians.

The stereophotogrammetric system, VECTRA M3 (Canfield Scientific Inc, Fairfield, USA) was used to collect facial data (Paragraph 1.2). As described in paragraph 1.4, before the acquisition of the faces, a set of 50 standardized landmarks was identified and marked on the patients' and controls' faces, using a black liquid make-up eyeliner [25,26].

The acquisitions were performed following a standardized procedure, with the subjects seated in front of the stereophotogrammetric system [27-30]. Once obtained the 3D facial reconstructions, all the landmarks were digitized on them. A subset was then chosen to extract the 3D coordinates and calculate a series of linear measurements.

The set of chosen landmarks included: Trichion (tr); Nasion (n); Pronasale (prn); Subnasale (sn); Christa philtri (cph); Pogonion (pg); Exocanthion (ex); Zygion (zy); Tragion (t); Gonion (go) (Figure 2.7).

Starting from the coordinates of these landmarks, 15 linear distances [mm] and 2 distances ratios [%] were calculated.

The measurements performed included

- horizontal distances: biocular width (ex_r-ex_l); skull base width (t_r-t_l); mandibular width (go_r-go_l); facial width (zy_r-zy_l); mouth width (ch_r-ch_l); philtrum width (cph_r-cph_l);
- vertical distances: length of the upper third of the face (tr-n); length of the middle third of the face (n-sn); length of the lower third of the face (sn-pg); morphological height of the face (n-pg); mandibular ramus length (t-go); mandibular body length (pg-go);
- sagittal distances: upper facial third depth (n-t); depth in the maxillary region (sn-t); mandibular sagittal plane depth (pg-t)
- ratios: posterior to anterior facial heights ratio (t-go/sn-pg); facial width/height (t-t/n-pg).

All the measurements were automatically calculated, using a custom software.

Z score values were then computed subtracting from the single measurement of each patient the corresponding mean measurement of the control group and dividing by the relevant standard deviation. Since by definition the average z score of control subjects is = 0 and its standard deviation is =1, all patient z scores outside the $\pm$ 1.5 interval were considered as clinically remarkable [27].

For patients younger than 18 years of age, the control group included subjects with the same age, patients older than 18 years were paired to controls with an interval span of a few years (18-25; 26-30 and 31-40 years). Once obtained, the single z score values of the patients, the mean z scores and their standard deviations were calculated for all measurements performed.

2.3 RESULTS

The comparison between DS patients and reference subjects did not reveal remarkable differences for the horizontal and sagittal distances (z score values comprised between -1.3 and 1.1). Nevertheless, among the vertical ones, the length of the patients' mandibular ramus (t-go) was reduced (z score = -1.7), with a consequent (even if not clinically relevant) reduction of the ratio between their posterior and anterior facial height (z score = -1.3).

Moreover, 4 of them had a reduction of the labial philtrum width (z scores respectively -0,9, -1,9, -2, -0,6), even if their mean z score was not outside the ±1.5 SD interval.

The limited sample dimension prevented from statistical considerations, but a different trend between males and females was observed for facial width and depth in the maxillary region: female faces were in the range of the controls, male ones were more different from controls.

The descriptive statistics of the z score values, calculated for the subjects are reported on tables 2.2 and 2.3.

2.4 DISCUSSION AND CONCLUSIONS

Misdiagnosis or absence of a correct diagnosis are common among DS patients. The phenotypical variability of this condition, together with the absence of a well-documented clinical history, collected from the disease beginning, often prevents from a correct clinical classification [50].

The identification of the disease, nevertheless, has a great importance both from a clinical and a familial point of view, since it allows the reduction of the seizures frequency, permitting a better quality of life for patients and their families [51].

This preliminary stereophotogrammetric assessment was performed with the aim of facilitating the recognition of the syndrome, even in adult patients, taking advantage of possible facial "soft markers" of the disease. In fact, many syndromes present a typical facial morphology, both during childhood and adulthood, that can be used to facilitate their identification [6,27-30].

In this context a 3D stereophotogrammetric assessment is advisable, being safe and fast and allowing the identification of facial features that can escape from a mere qualitative, though expert, evaluation [20].

A first attempt to evaluate the facial morphology of DS patients was performed by Nolan et al. in 2011, analysing, through a series of linear measurements the photographic records of a group of

12 DS patients of age comprised between 4 and 12 years. Data coming from siblings were used as control. Statistical significant differences were not found for the measurements analysed between patients and their relatives [52].

Conversely, from our preliminary results patients show an average reduction of their mandibular ramus length, a consequent reduction of the ratio between the posterior and anterior facial heights and the presence, for four of them, of a reduction of the labial philtrum width (typical facial feature of different syndromic conditions) (Figure 2.8).

The different study design and the different used technologies explain the contrasting results. Nonetheless, the identification of dysmorphic features among adult DS patients encourages the performance of further studies on a larger sample, providing a stronger statistical value to the results and maybe pointing out a role of SCN1A in facial morphogenesis.

2.5 Study 2: 3D Craniofacial morphometric analysis of GLUT-1 DS patients.

Glut1 deficiency syndrome (GLUT1-DS, OMIM #606777; ORPHA:21772) is a neurological and metabolic disorder caused by a defective transport of the glucose across the blood brain barrier (BBB).

Early defined as an epileptic encephalopathy of the child and classified as “classical” and “non-classical”, according to the type of epilepsy manifested, it is currently considered a spectrum, which includes, together with epilepsy, movement disorders, language problems, mental retardation and other paroxysms. Microcephaly and prognathism have been described for what concerns craniofacial characteristics of the patients [53-58].

The syndrome is caused by *de novo*, autosomal dominant, or sporadic mutations on the gene SCL2A1 (1p35-31.3), that encodes for the glucose transporter type 1 and, when mutated, does not allow the glucose to go through the BBB, to be used as an energy source [57,59,60].

Lumbar puncture is currently used to diagnose this condition, thus allowing researchers to reveal the presence of low levels of glucose in the cerebrospinal fluid, in a general context of normoglycemia; molecular analysis of the gene can be performed for confirmation. The variability of the symptoms, nevertheless, often makes the diagnosis very difficult [55,58,61].

Since patients sometimes do not respond to the classic antiepileptic drugs, GLUT1-DS elective treatment is at the moment based on the ketogenic diet, to provide an alternative energy source to the brain and reduce seizures and paroxysm frequency [62,63].

In order to favour a prompt individuation of the disease and a correct diagnosis, the aim of this study is to perform a stereophotogrammetric study of facial size and shape variations of GLUT1-DS patients, using multivariate statistical techniques [27,57,64].

The study is encouraged by the previous observations of a tendency to prognathism in a group of Italian patients, recently confirmed by a pilot study executed by our group [28,57].

2.6 MATERIALS AND METHODS

The sample was composed of 216 subjects and included 11 female patients of age comprised between 3 and 32 years and 205 female controls of the same age as patients. All the patients had received a genetic diagnosis and were unrelated, except for a couple mother/daughter. Eight of

them presented missense mutations, two had nonsense mutations and 1 of them had a deletion. Neither patients nor controls had a previous history of facial surgery or facial trauma (Table 2.4).

Patients and controls were imaged through the stereophotogrammetric system VECTRA M3 3D (Canfield Scientific Inc. Fairfield, NJ, USA) (Paragraph 1.2); the acquisitions were performed according to the protocol described in paragraph 1.4. Although not invasive, all the procedures were executed after the signature of an informed consent and after the approval by the ethics committee of Università degli Studi di Milano, 27 June 2014, no.266 230 92/2014, in accordance to the tenets of the Declaration of Helsinki.

Among the 50 landmarks defined by the laboratory protocol for facial morphometric analysis, 42 were used to investigate GLUT-1DS facial morphology. In particular, all the facial landmarks were considered, except for those located on the ears [25,26] (Figure 2.9).

From the single reference points x, y and z coordinates were extracted, both for patients and controls, in order to calculate landmark-to-landmark anthropometric measurements (and their z scores) and to perform a Principal Components Analysis (PCA).

Anthropometric measurements

Starting from the three-dimensional coordinates of the chosen landmarks, linear distances, angles, areas and ratios, indicated in table 2.5, were computed, both for patients and controls.

Patients' measurements were transformed into z scores using means and standard deviations, calculated from the corresponding measurements of the reference group [65]. A paired Student t test, with a statistical significance level set at $p < 0.05$, was used to compare average z scores of the patients and controls.

Principal Components Analysis

The set of 42 anthropometric landmarks considered both for patients and control subjects was used to create some points clouds, superimposed through a preliminary procrustes registration, in order to adjust translational, rotational and isometric scaling data components.

A principal Component Analysis (PCA) was then executed using Matlab (Mathworks, Natick, USA), in order to quantify the differences between the faces of GLUT-1DS patients and corresponding control subjects.

PCA permitted to calculate some derived variables, called principal components (PCs), that represent a linear combination of the original variables and describe the axes of shape variation [66].

Stepwise regression was then used to identify a subset of the aforementioned PCs, indicative of the morphological differences between GLUT1-DS and control subjects facial features. The level of statistical significance was set at $p<0.05$.

2.7 RESULTS

Anthropometric measurements

The analysis of the z scores revealed that patients have peculiar features localised in the ocular and mandibular regions: in particular the eyes are smaller, closer and down-slanted in comparison to the control subjects. They also present a reduction in the facial depths, at the level of middle and lower facial thirds, with a particular involvement of the mandibular area. Nevertheless, their mandibular body is longer compared to the controls and the sn-t/ pg-go ratio results reduced. The mandibular ramus appears shorter, with a consequent reduction of the anterior to posterior facial heights ratio in comparison to controls.

For what concerns the angles, their mandibular convexity and facial divergence result increased, while the lower facial convexity decreased in comparison to reference subjects. Also mandibular angles are smaller than those of the controls.

Table 2.6 illustrates the mean z scores, their standard deviations (SD) and the p values for the measurements calculated in the current study. Figures 2.10 and 2.11 show a graphical representation of the statistically significant z scores of the patients, divided for the anatomical district considered.

Principal components analysis

From the 216 point clouds representing all the subjects, and each one constituted by 42 facial landmarks defined in the 3D space, the PCA allowed the calculation of 126 PCs.

Among them, the first 22 described 90% of facial variability in the sample, while 99% of variability was described by the first 71 PCs.

Twenty-three PCs were retained to perform a stepwise regression (Table 2.7). Furthermore, in order to investigate the role of these components in facial morphology, PC1, PC2 and PC9, which were the three most significant PCs, were selected.

Once defined a 3D space, through these 3 components, GLUT1-DS patients were all clustered in the negative parts, showing a more homogeneous distribution than reference subjects (Figure 2.12).

Forty-four percent of the total variance could be explained by PC1, with the bigger variations located in the upper and lower parts of the face. GLUT1-DS patients (average configuration minus 1.96 SD, Figure 2.13a) showed a high forehead, smaller eyes and a prominent nose; a short mandibular ramus with a long mandibular body, small gonial angles and a reduced chin prominence.

Nine percent of the total variance was explained by PC2 and confirmed the presence, for Glut1-DS patients, of a high forehead, smaller eyes, and reduced chin prominence (average configuration minus 1.96 SD, Figure 2.13b). Furthermore, it was possible to appreciate a reduced facial depth with an increased facial divergence.

Modifications included in PC9 (2% of total variance) regarded the mouth, with an increased lip prominence and a reduced chin prominence (average configuration minus 1.96 SD, Figure 2.13c).

2.8 DISCUSSION AND CONCLUSIONS

The heterogeneity of the symptoms and the presence of familiar epilepsies with mental and motor impairment makes the diagnosis of GLUT-1DS arduous [67], thus delaying the introduction of the ketogenic diet that should be given as soon as possible and maintained until adolescence [68]. An early diagnosis is therefore necessary to start the treatment, trying to keep seizures under control.

The necessity to favour an early diagnosis, the presence of previous qualitative observations describing, for a group of Italian patients a tendency to prognathism, together with the preliminary results of a facial morphometric analysis conducted by our group, encouraged this study which was aimed at performing a more complex morphometric assessment, through conventional anthropometric measurements and PCA [28,57].

Conventional anthropometric measurements and, in particular z scores find a wide application in medicine, especially to the analysis of anomalies in foetal ultrasonography. PCA, on the other

hand, represents a strong multivariate statistical method to assess the variability of spatial data, whose application has a potential role in the early recognition of syndromes and diseases [64,69].

In this study the results of conventional anthropometry were in accordance with PCA. Patients seemed to have more homogeneous faces compared to controls. Most of the anomalies were on the forehead (increased), eyes (decreased), nose (prominent), middle and lower facial width and depth (decreased), and the mandible (longer mandibular body and shorter ramus, small gonial angles, reduced chin prominence, increased lip prominence, increased facial divergence). It has to be mentioned that the facial configurations shown in figure 2.13 do not necessarily represent actual faces, but they are mathematical tools that allow the focus over the major characteristics of the patients.

The identification of typical facial features, common among GLUT1-DS patients, could have a role in increasing the knowledge of the pathology itself and its cellular and molecular bases. An experimental animal model of this disease was proposed by Jensen et al. It permitted to demonstrate that the silencing of glut1 orthologue in zebra fish caused an impaired cerebral organogenesis, restored by the human transporter mRNA expression [70].

Even if this experimental model could not perfectly mimic what exactly happens in humans, because they maintain a functional copy of the gene, it is important to remember that, embryologically, the face and the brain are mutually connected and alterations to the cerebral development, due to genetic mechanisms, could manifest in abnormal facial characteristics [30,71,72].

In the current study, the modifications found in the upper facial parts of the patients may be connected to an impaired brain development, as seen in forebrain pathologies [30].

Furthermore, the alterations localised in the mandibular area sustained the presence of prognathism, qualitatively described for these patients.

Indeed, recent studies performed in prognathic subjects, found a set of genes related to the excess of mandibular prominence on chromosome 1 (1p36; 1p22.3; 1p22.1; 1q32.2). These genes were located next to the genetic region altered on GLUT1-DS patients (1p35-31.3). This association may possibly clarify the connection between the two disorders by a genetic linkage and explain the facial phenotype observed in these patients [73-75].

In conclusion, even if a facial morphometric analysis cannot substitute the clinical and genetic diagnosis, its safety and low costs permit its use as a first screening test to suspect the presence of this syndrome and to evaluate possible longitudinal craniofacial modifications.

Furthermore, the knowledge of the specific facial features of the patients can be advantageous for a better management of orthodontic and orthopaedics treatments that patients may perform [76].

2.9 Study 3: Stereophotogrammetric analysis of a case of holoprosencephaly.

Holoprosencephaly (HPE, OMIM #236100) is a congenital brain malformation, due to an incorrect development of the hemispheres of the forebrain and the lateral ventricles during embryonic development, also characterized by the loss of the midline brain structures [77-81]. It is present in 1 out of every 250 pregnancies, but only 1/8000- 1/10000 fetuses survive [77,80,82]. It is generally classified in 3 subtypes (alobar, semilobar and lobar) depending on the symptoms severity and includes a less severe variant called the middle inter- hemispheric variant (MIH).

Craniofacial deformities involve 80% of the cases and include cyclopia, premaxillary agenesis or synophtalmia, ethmocephaly or cebocephaly, agenesis of nasal bones, median cleft lip and palate, single maxillary incisor and hypotelorism and manifest together endocrine digestive and respiratory problems [77,78,83-86]. Epileptic seizures and developmental and mental retardation may complete the clinical picture [87]. The pathogenesis of the disease includes genetic (in less than 5% of the cases) and environmental factors [88], including maternal diabetes and the consumption of some drugs (like salicylates), alcohol abuse, low levels of cholesterol and sexual or respiratory infections. [78,88]. The diagnosis relies on foetal ultrasonography, but MRI can provide further details for the disease recognition [89-92].

In this study, it is described the 3D stereophotogrammetric analysis of the facial morphology of a 2-year-old girl affected by lobar HPE and epilepsy, that at the first observation, presented a nearly normal face. According to the classic presence of facial dismorphism in HPE cases, the 3D facial analysis allowed the individuation of several typical abnormal characteristics.

The diagnosis of HPE was done at the 27^{th}week of pregnancy, through ultrasonography and showed the union of the frontal horns of the lateral ventricles and the incomplete presence of the inter-hemispheric fissure, in the absence of the septum pellucidum and the corpus callosum. It

was executed in accordance to the flowchart proposed by Malinger et al. for differentiation of HPE from similar conditions [93]. Foetal MRI was later performed and sustained the previous diagnosis of lobar HPE.

The girl was born at the 38^{th}+6 weeks of pregnancy, with a physiological and regular vaginal delivery. At birth, her weight was 2860 g, she was 47 cm long, with a head circumference of 33 cm. All measurements were between the 10^{th} and 25^{th} percentiles; Apgar score was 9/10.

The girl had 2 healthy brothers of 3 and 4 years of age. Their parents were non-consanguineous, healthy and had an age of 30 years at her birth. Familiar history did not include neurological disorders and syndromes. HPE, even microforms, was excluded for them. Furthermore, the mother did not have risk factors, except the consumption of ketoprofen in the first weeks of pregnancy and the sporadic consumption of low alcohol doses.

The facial aspect of the girl was nearly normal apart from synophrys and skin appendages, located between the anterior notch and the intertragic incisure of each ear (Figure 2.14).

Postnatally, the diagnosis was confirmed by other MRIs, and revealed an altered cortical cyto-architecture, pachygyria, partial interhemispheric fronto-parietal fusion and a single ventricular cavity (third and lateral ventricles) in the absence of cerebellar and brainstem alterations (Figure 2.15). Genomic DNA sequences were investigated through a comparative genomic hybridisation array (CGH), which did not reveal variations in the number of copies. The levels of 7-dehydrocholesterol were normal. The girl is currently taking antiepileptic treatment and thyroid replacement therapy. She also follows a support ketogenic diet. Before this study, no one had ever investigated her craniofacial assessment.

2.10 MATERIALS AND METHODS

A stereophotogrammetric facial analysis of the patient and her mother was executed. Both of them were Caucasoid and did not have a previous history of facial trauma or surgery. All procedures had received the approval by the local ethics committee and were performed in accordance to the tenets of the Declaration of Helsinki.

The subjects were imaged using the stereophotogrammetric system (VECTRA M3, 3D Canfield Scientific Inc., Fairfield, NJ, USA), described in paragraph 1.2, following the landmarking protocol already described in detail in literature and reported in paragraph 1.4 [94]. During the

stereophotogrammetric acquisition the child was seated on her mother's lap and was not able to keep her mouth closed.

Geometric models of the subjects' faces were reconstructed from the coordinates of the landmarks identified, in order to calculate a set of linear distances (Figure 2.16, Table 2.8).

Reference values from a sample of 123 paired healthy controls were used to calculate the z score values of the patient; while 200 healthy control women were used to calculate the reference values for the mother. All values that were more than 1.5 standard deviations different from the control subjects were further analysed.

2.11 RESULTS

Figures 2.17-2.19 show the z score values calculated for child distances respectively on the vertical, horizontal, and sagittal planes, and the comparison with the relevant values calculated for her mother. Additionally, z score values of the patient and her mother that differ 1.5 SD or more from the reference values are listed in table 2.9.

A reduction of the forehead height (z score -3.7) determined a shorter face of the patient compared to controls, while the other distances in the vertical plane were similar to the reference subjects. The open mouth position was maybe responsible for the increased length of the lower facial third.

The skull base, mandibular and facial widths were increased compared to controls (all z scores larger than 3). All these values were normal in the mother, except for a subtle reduction of the skull base width and an increased height of the chin.

Both mother and child had reduced horizontal dimensions of the eyes, with the child having z scores larger than 3.5, together with increased ocular vertical dimensions, a slightly reduced biocular width (z score -1.8) and increased intercanthal width (z score 1.8).

The patient face was quite flat, with a shorter nasal bridge compared to reference subjects, reduced depth of the supraorbital rim, orbito-tragial distances, depth of the upper third of the face and depth in the maxillary and mandibular regions (z scores comprised between -1.6 and -4), despite the presence of an increased right-side depth of the lower jaw.

Some of these characteristics were shared with the mother, including the reduced nasal bridge length, right-side depth of the supraorbital rim, orbito-tragial distances and depths in the maxillary and mandibular regions. In common with the mother, the girl also presented a larger labial philtrum (z score for both 2.3). For a comparison of the craniofacial characteristics of the mother

and her daughter, a correlation analysis between their paired z scores was executed. The resulting r was = 0.51.

2.12 DISCUSSION AND CONCLUSIONS

The presence of a normal facial appearance for people affected by HPE is possible, as reported in literature [95].

For the girl analysed in the current study, the diagnosis of HPE was performed at the 27th week of pregnancy through ultrasounds. Ultrasonography, indeed, is an appropriate tool for prenatal HPE diagnosis, even if magnetic resonance imaging is the main diagnostic technique [92,96,97].

The current patient, despite lobar HPE, presented, at a first glance, a normal appearance except for appendages on both ears and synophrys (Figure 2.14), in contrast with the paradigm sustained by De Meyer et al., that "The face predicts the brain" in patients with HPE [98]. Nevertheless, the 3D facial stereophotogrammetric analysis revealed that most of the facial distances evaluated in the girl were different from those of the controls, thus again confirming the aforementioned paradigm [98].

The development of the face and the brain is indeed connected and they influence each other: the facial characteristics of patients with HPE can result from the impairment of the prosencephalic organizing center, which may arise from defective mutual relationships among brain, neural crest cells and surface ectoderm [99,100]. Moreover, the growth of the skeletal and nervous system is related and nervous developmental defects can affect the bony structure [85].

For this reason, the knowledge of facial morphology is important in understanding the embryological origin of the affected facial and cerebral structures, in order to establish the timing of the existing defects, compare the level of osseous and cerebral involvement and increase the basic knowledge about this condition [85].

Even if a facial morphometric analysis will never substitute a radiological diagnosis, it permits the identification of facial features related to this condition. It also allows an objective and quantitative assessment of not immediately evident dysmorphic features, whose recognition can provide details on the underlying pathology, maybe helpful, in the future, for the clinic diagnosis.

The facial features of the patient and her mother were compared to those of control subjects through z scores. These values find a wide application in anthropometry, maxillofacial surgery and ultrasonography, to identify the presence of genetic syndromes [3,101]. The mother/child comparison was also aimed at identifying familiar traits, possibly independent from the pathology.

The facial features of the girl comprised a reduction in facial length (short forehead and a wider face) never described in literature (Figures 2.17-2.19), together with a reduction in the horizontal and an increase in the vertical ocular dimensions.

Her biocular width was reduced, in accordance with the typical hypotelorism of patients with HPE, while the reduced length of the ocular fissure can be a familiar tract, as it was found in the mother, too [102].

On the other hand, the presence of a flat face is in accordance with the literature that indicates in these patients' flat noses and hypotelorism [78, 103-105]. Moreover, literature describes a larger labial philtrum, as associated with several syndromes, even if in this case it maybe a familiar tract [106,107].

The etiology of HPE has not been completely clarified, however, for this patient, the genetic analysis was negative, but teratogenic substances (alcohol and salycilates) were consumed by the mother, even if in low quantities. The first one has already been described as a risk factor, while reports about the second are not available in literature [78]. For what concerns alcohol consumption, its role has been investigated in mutant mices, exposed in utero to alcohol, thus demonstrating its causative role in genetically predisposed individuals [108]. In this patient, gene sequencing was not performed, but, a genetic predisposition may have had a role in the susceptibility of the girl to alcohol consumption during gestation [109].

It is important to note that all the features found altered in the upper part of the girl's face are compatible with a forebrain dysmorphogenesis like HPE [110]. Indeed, dysmorphogenesis of the frontonasal and adjacent facial areas, that has in common with the forebrain embryological gene expression domains, has already been related to alterations in anterior cerebral regions [111]. Since this investigation reports altered facial features which have never been described before, together with already known characteristics, it sustains the importance of facial morphometric analysis with stereophotogrammetry. Further studies involving a larger number of patients are advisable.

Table 2.1. Patients analysed in study 1 and number of corresponding control subjects used for comparisons [112].

	gender	age (years)	# of reference subjects
patient #1	female	16	30
patient #2	female	17	13
patient #3	female	26	23
patient #4	male	18	178
patient #5	male	32	76
patient #6	male	37	76

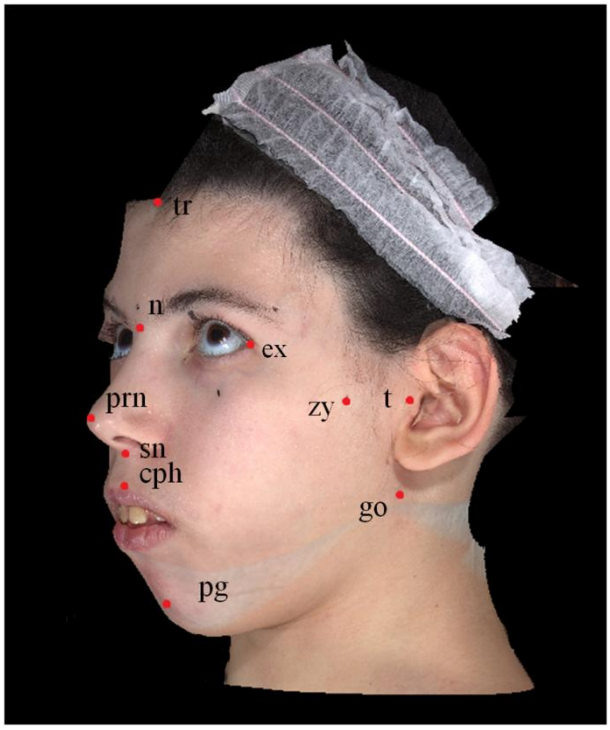

Figure 2.7. Landmarks digitized on a patient's face (Study 1). All the landmarks have been digitized on all subjects [112].

Table 2.2. Descriptive statistics of the z scores calculated for horizontal and vertical distances of study 1. Measurements differing on average 1.5 SD or more from the reference values are marked with ***** [112].

	ex_r-ex_l	**t_r-t_l**	**go_r-go_l**	**zy_r-zy_l**	**ch_r-ch_l**	**tr-n**	**cph_r-cph_l**	**n-sn**	**sn-pg**	**n-pg**	**t-go**
F1	-0.2	0.3	0.3	-0.1	-0.1	-0.6	2.1	0.9	-0.7	0.3	-2.9
F2	-0.1	-0.1	0.6	0	0.3	-1	-0.9	-0.8	0.8	0	-1.6
F3	0.2	0.2	0.3	0.1	-0.7	1.8	-1.9	0.1	1.4	0.5	-1.4
M1	-0.8	-0.8	-0.3	-3.2	-0.9	-0.3	-2	0.2	-0.6	0	-0.9
M2	-3	-1.2	1.9	-2.3	-1.2	-0.2	0.1	1.2	0.1	1.2	-2
M3	-0.8	-3	-0.6	-1.6	0.7	-1.5	-0.6	-1.1	1.5	0.4	-1.7
Mean	*-0.8*	*-0.8*	*0.4*	*-1.2*	*-0.3*	*-0.3*	*-0.5*	*0.1*	*0.4*	*0.4*	*-1.7**
SD	*1.1*	*1.3*	*0.9*	*1.4*	*0.8*	*1.1*	*1.5*	*0.9*	*1*	*0.4*	*0.7*
Min	*-3*	*-3*	*-.,6*	*-3.2*	*-1.2*	*-1.6*	*-2*	*-1.1*	*-0.7*	*0*	*-2.9*
Max	*0.2*	*0.3*	*1.9*	*0.1*	*0.7*	*1.8*	*2.1*	*1.2*	*1.5*	*1.2*	*-0.9*

Table 2.3. Descriptive statistics of the z scores calculated for sagittal distances and ratios of study 1 [112].

	pg-go	n-t	sn-t	pg-t	t-go/sn-pg	t-t/n-pg
F1	2	0	0.1	0.2	-1.3	-0.4
F2	0.9	-0.6	-0.8	-1.1	-1.6	-0.1
F3	1.8	0.3	0.3	0.3	-1.8	-1.1
M1	0	-1	-2.6	-2.2	-0.7	-0.5
M2	0.9	-0.6	-1.7	-1.3	-1	-1.6
M3	0.7	-1.6	-2	-2.6	-1.3	0
Mean	*1.1*	*-0.6*	*-1.1*	*-1.1*	*-1.3*	*-0.6*
SD	*0.7*	*0.7*	*1.2*	*1.2*	*0.4*	*0.6*
Min	*0*	*-1.6*	*-2.6*	*-2.6*	*-1.8*	*-1.6*
Max	*2*	*0.3*	*0.3*	*0.3*	*-0.7*	*0*

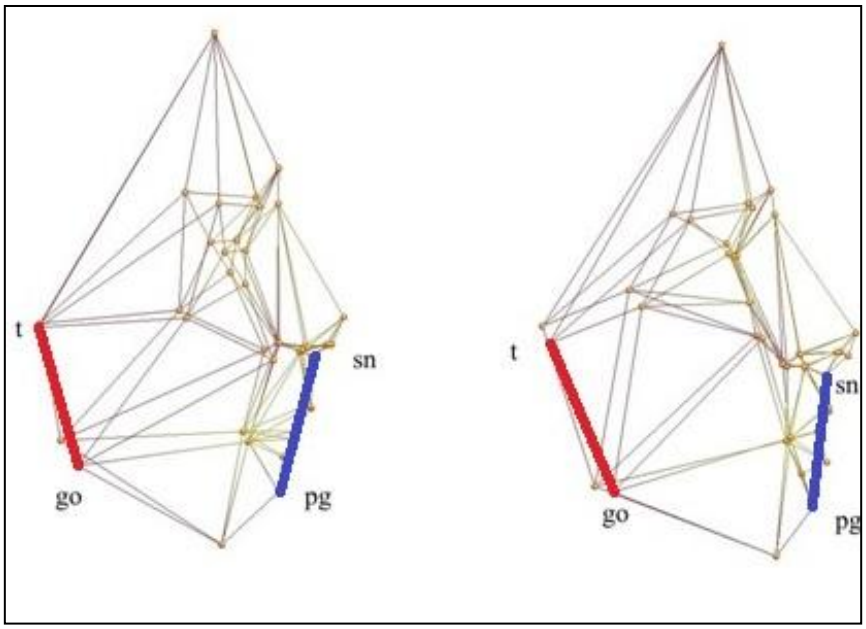

Figure 2.8. Left: geometric representation of the average profile of the patients; right: geometric representation of the average profile of the controls, T-Go: mandibular ramus length (posterior facial height, in red); Sn-Pg: anterior facial height, in blue (study 1) [112].

Table 2.4. Patients involved in study 2 and their mutations. Patient #1 and 2 are related [32].

Patient#	Sex	Age (years)	Protein Mutation	Type of mutation
1	female	11	V165I	Missense
2	female	32	V165I	Missense
3	female	29	R126C	Missense
4	female	14	p.Thr295Met /pT295M9	Missense
5	female	27	W48X	Nonsense
6	female	18	c.457C>T	Missense
7	female	8	p.N34S	Missense
8	female	3	R249Afs131X	Nonsense
9	female	17	p.Arg 400 cys	Missense
10	female	8	p.Leu124TrpfsX12	Deletion
11	female	10	R153C	Missense

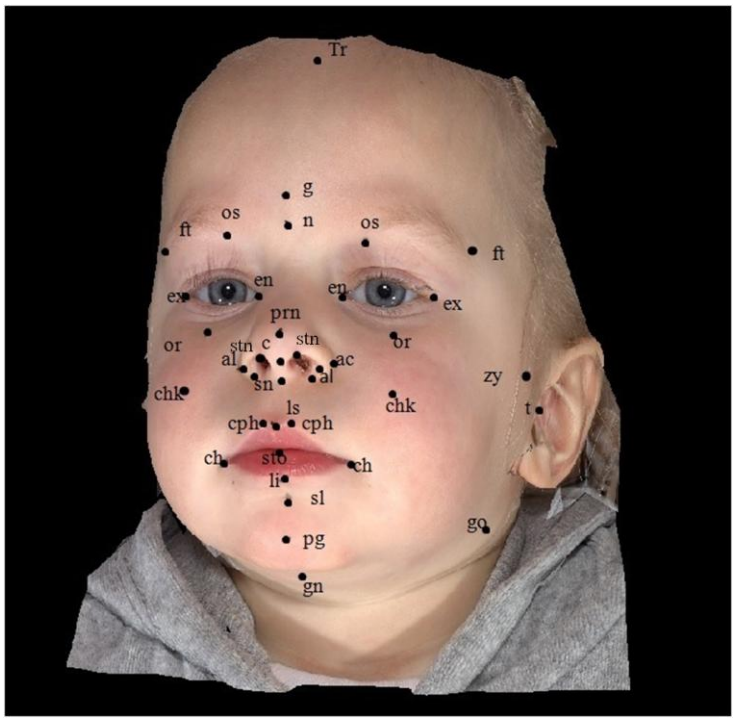

Figure 2.9. Anthropometric landmarks identified on a study 2 patient's face [32].

Table 2.5. Anthropometric measurements performed in study 2. a) distances; b) angles; c) areas and ratios [32].

a) Distances [mm]	
Intercanthal distance	ex-ex
Middle facial width	t-t
Lower facial width	go-go
Ocular width (right and left)	en-ex
Mouth width	ch-ch
Forehead height	tr-n
Height of the nose	n-sn
Lower facial height	sn-pg
Total facial height	n-pg
Upper facial depth	n-t
Middle facial depth	sn-t
Lower facial depth	pg-t
Mandibular corpus length	pg-go
Mandibluar ramus length	t-go
Width of the face	zy-zy

b) Angles [°]	
Sagittal convexity (excluding nose)	n-sn-pg
Sagittal facial convexity (including nose)	n-prn-pg
Midfacial to mandibular plane	(t-n)-(pg-go)
Inclination of the eye fissure versus the true horizontal	en-ex^THR
Maxillary prominence	sl-n-sn
Mandibular convexity	go-pg-go
Gonial angle (right and left)	t-go-pg
Lower facial convexity	t-pg-t

c) Areas [cm^2]	Ratios [%]	
Soft-tissue ocular area (right and left)	Facial width/ total facial height ratio	t-t/n-pg
	Middle/lower facial depth ratio	sn-t/pg-t
	Middle facial depth/ mandibular corpus length ratio	sn-t/pg-go
	Posterior/anterior facial height ratio	t-go/sn-pg

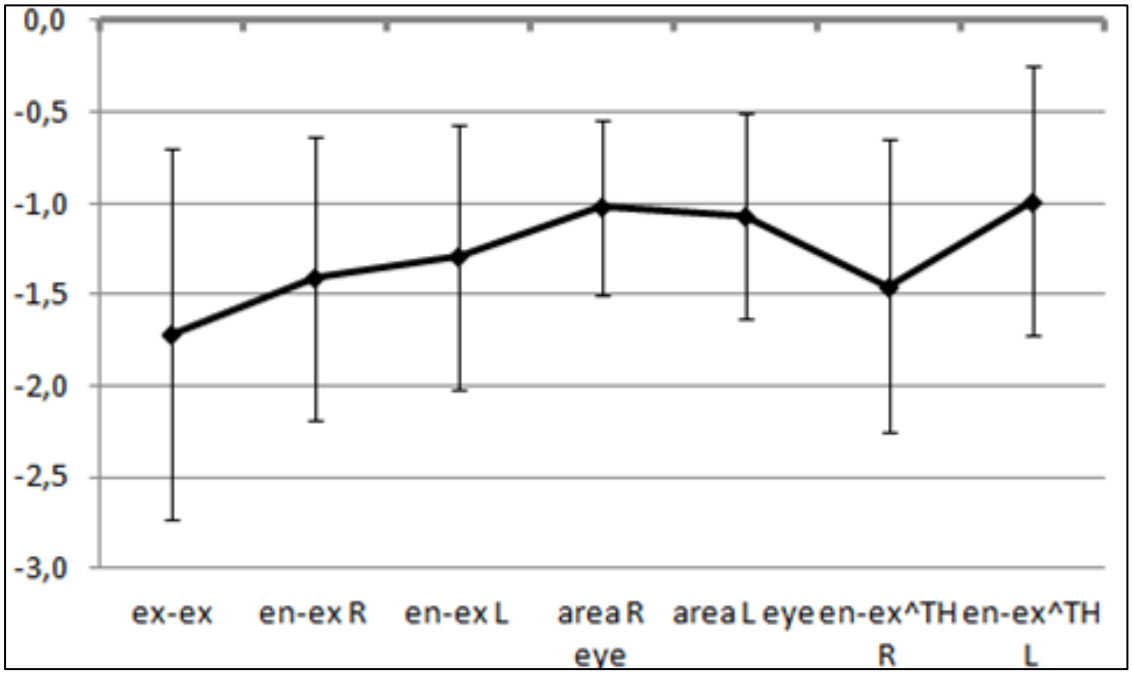

Figure 2.10. Statistical significant z-score values of the eye region (mean ± 1 SD). Continuous line indicates the reference z-score of the controls, that by definition is 0 (study 2) [32].

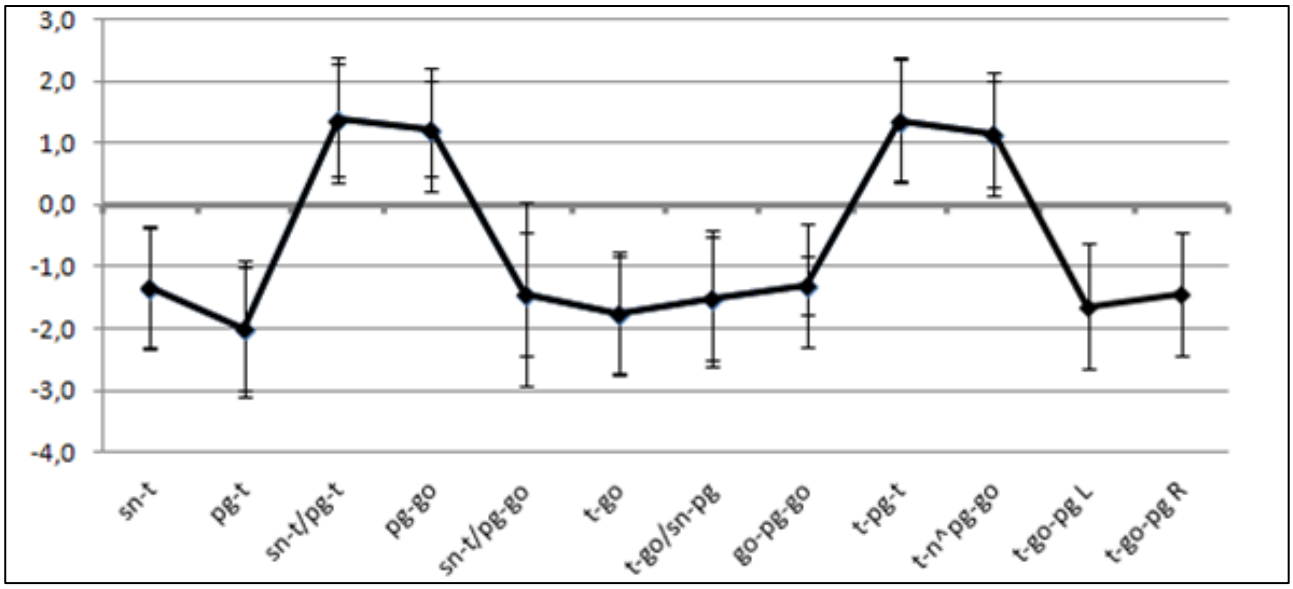

Figure 2.11. Statistical significant z-scores values of the mandibular region (mean ± 1 SD). Continuous line indicates the reference z-score of the controls, that by definition is 0 (study 2) [32].

Table 2.6. Mean, standard deviations (SD) and p-values of the anthropometric measurements performed (study 2)[32].

		Mean	**SD**	**p-value**			**Mean**	**SD**	**p-value**
Distances [mm]	**ex-ex**	-1.712	1.013	< 0.01	**Angles [°]**	**n-sn-pg**	-0.694	0.646	< 0.01
	t-t	-0.633	0.939	0.05		**n-prn-pg**	-0.224	0.544	0.201
	go-go	0.360	0.803	0.168		**(t-n)-(pg-go)**	1.143	0.856	< 0.01
	en-ex	-1.407	0.777	< 0.01		**en-ex^THR**	-1.453	0.801	< 0.01
	en-ex	-1.291	0.721	< 0.01		**en-ex^THR**	-0.984	0.740	< 0.01
	ch-ch	-0.506	1.427	0.267		**sl-n-sn**	0.483	0.798	0.072
	tr-n	-0.129	1.651	0.801		**go-pg-go**	-1.300	0.479	< 0.01
	n-sn	0.686	1.156	0.077		**t-go-pg**	-1.439	0.878	< 0.01
	sn-pg	0.186	1.591	0.707		**t-pg-t**	1.372	0.968	< 0.01
	n-pg	0.478	0.907	0.111	**Ratios [%]**				
	n-t	-0.650	0.941	0.045		**t-t/n-pg**	-0.822	0.923	0.014
	sn-t	-1.333	0.969	< 0.01		**sn-t/pg-t**	1.376	0.909	< 0.01
	pg-t	-1.986	1.096	< 0.01		**sn-t/pg-go**	-1.427	1.485	0.01
	pg-go	1.225	0.764	< 0.01		**t-go/sn-pg**	-1.522	1.103	< 0.01
	t-go	-1.764	0.945	< 0.01	**Areas [cm^2]**	**Soft-tissue ocular area right**	-1.019	0.477	< 0.01
	zy-zy	-0.649	1.242	0.113		**Soft-tissue ocular area left**	-1.063	0.564	< 0.01

Table 2.7. Coefficient values of the PCs included in the regression model and the corresponding t and p-values (study 2) [32].

	Coefficients	**t-value**	**p-value**
PC 1	-0.002	-5.921	$1.5 \cdot 10^{-8}$
PC 2	-0.005	-7.277	$8.5 \cdot 10^{-12}$
PC 3	-0.002	-2.635	$9.1 \cdot 10^{-3}$
PC 6	0.006	5.150	$6.4 \cdot 10^{-7}$
PC 9	-0.009	-5.695	$4.6 \cdot 10^{-8}$
PC 11	0.004	2.532	0.012
PC 13	-0.006	-2.876	0.005
PC 14	-0.005	-2.595	0.012
PC 21	-0.011	-4.062	$7.1 \cdot 10^{-5}$
PC 22	0.008	2.856	0.005
PC 23	-0.007	-2.208	0.028
PC 34	-0.009	-2.234	0.027
PC 36	-0.016	-3.637	$3.5 \cdot 10^{-4}$
PC 41	-0.013	-2.539	0.012
PC 47	-0.012	-2.004	0.046
PC 59	-0.018	-2.383	0.018
PC 66	0.019	2.117	0.036
PC 71	0.026	2.606	0.009
PC 86	-0.039	-2.754	0.007
PC 95	-0.055	-3.027	0.003
PC 100	0.051	2.430	0.016
PC 113	-0.105	-2.856	0.005

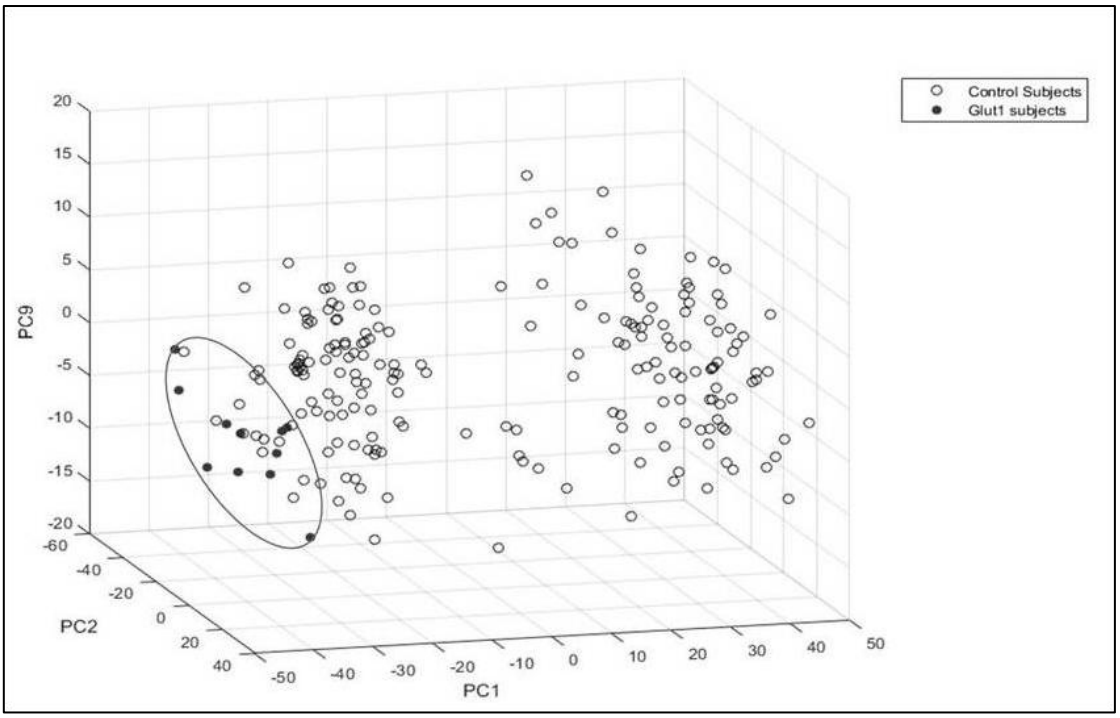

Figure 2.12. Comparison of Glut1-DS and control subjects in the principal component space, defined by the three more significant components included in the regression model. The ellipse highlights how the Glut1-DS subjects are distributed (study 2) [32].

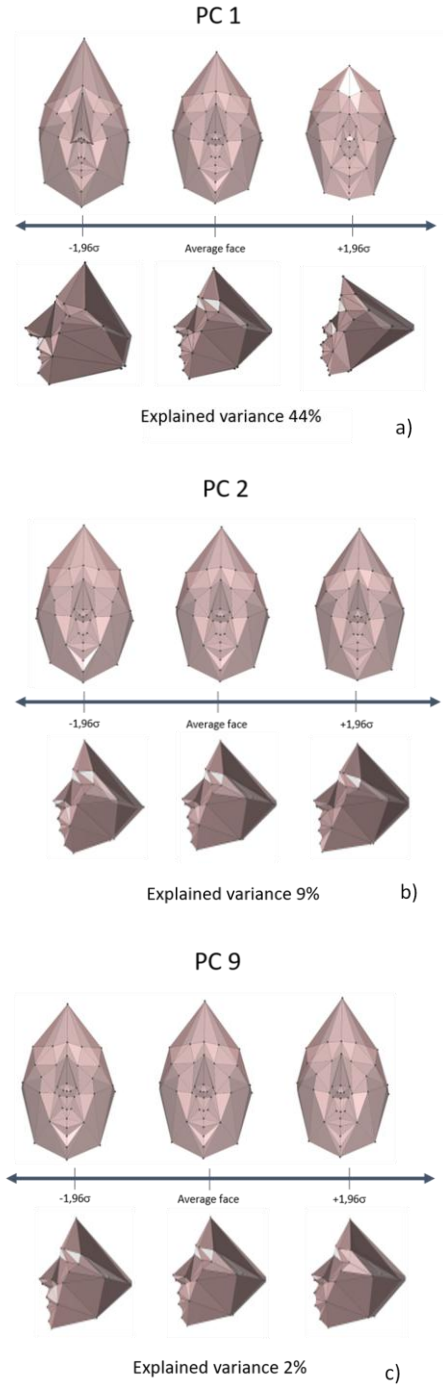

Figure 2.13. (a-c).Effect of the variation of the three most significant PCs included inthe regression model. For each PC, the average configuration, and those differing 1.96 SD, are depicted (study 2) [32].

Figure 2.14. Frontal photograph of the 2-year-old child with HPE, showing an apparent normal facial aspect, except for the presence of synophrys. b) Left ear, showing the skin appendage on the tragus (study 3) [30].

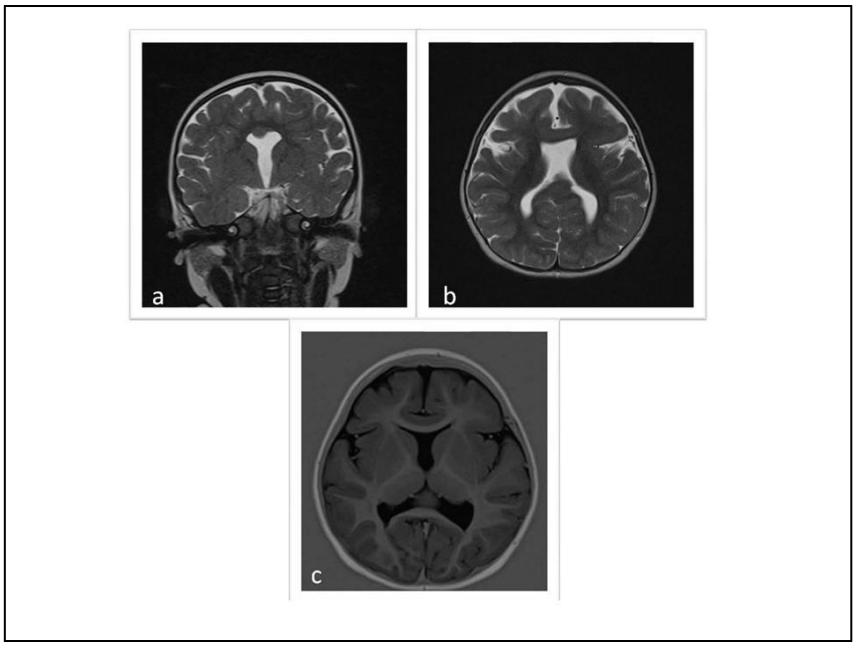

Figure 2.15. MRI: a) coronal, b) transversal T2 , c) transversal T1 images. The images show a partial fusion of the ventricular system, cortical pachigiria, frontal and temporal lobe atrophy, agenesis of corpus callosum with minimal preservation of rostrum (study 3) [30].

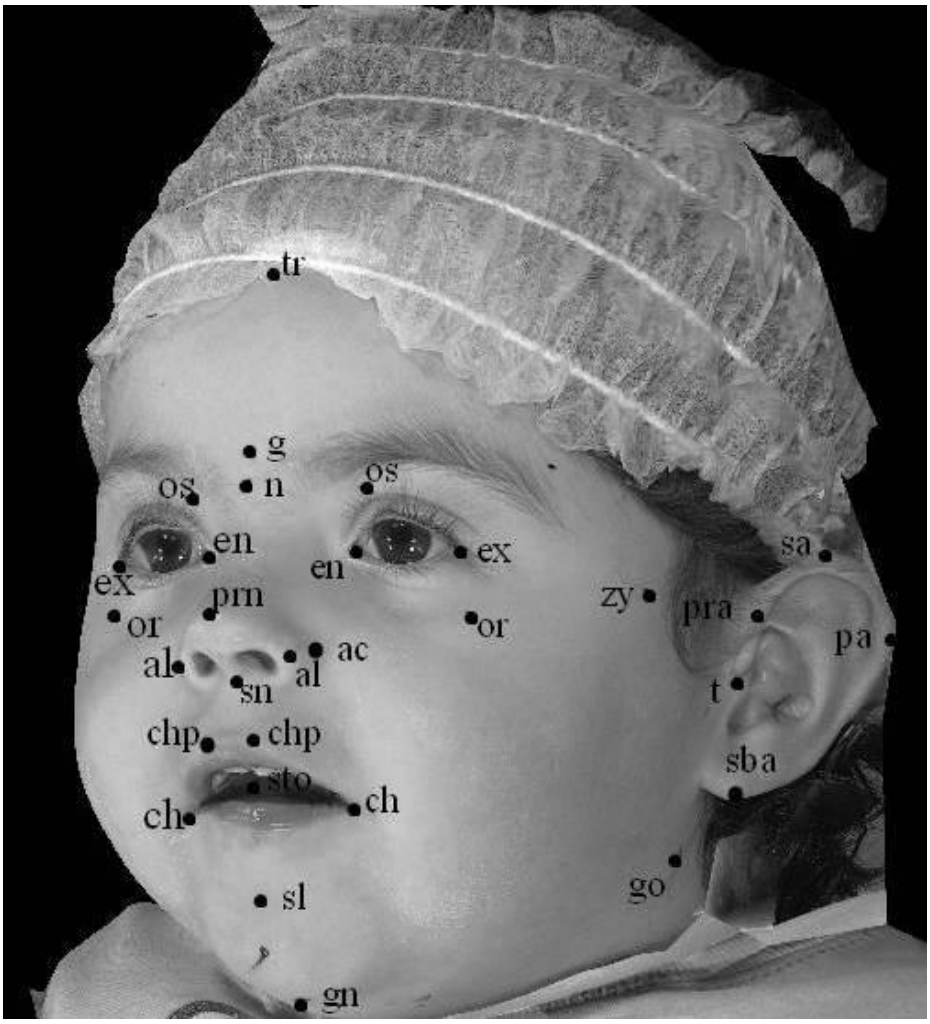

Figure 2.16. Three-quarter photograph of the child and analysed landmarks. trichion: tr; glabella: gl; nasion: n; pronasale: prn; subnasale: sn; stomion: sto; sublabiale: sl; gnathion: gn; exocanthion: ex; endocanthion: en; orbitale superius: os; orbitale:or; alare:al; nasal alar crest: ac; crista philtri: chp; cheilion: ch; zygion: zy; tragion: t; gonion: go; preaurale: pra; superaurale: sa; postaurale: pa; subaurale: sba (study 3) [30].

Table 2.8. Linear distances calculated in study 3 [30].

Plane	**Distances (mm)**		**Location**
Vertical	tr-n	height of the forehead	Upper face
	tr-gn	physiognomical height of the face	Face
	n-gn	morphological height of the face	Face
	n-sn	height of the nose	Face
	os-or	vertical dimensions of the eye	Eyes, paired
	n-prn	nasal bridge length	Face
	sn-gn	length of the lower facial third	Face
	n-sto	physiognomical height of the upper face	Face
	sl-gn	height of the chin	Lower face
	sa-sba	ear length	Ear, paired
Horizontal	ex-ex	biocular width	Eyes
	en-en	intercanthal width	Eyes
	ex-en	length of the ocular fissure	Eyes, paired
	zy-zy	width of the face	Face
	al-al	nasal width	Nose
	ac-ac	width between the facial insertion points of the alar base	Nose
	t-t	width of the skull base	Face
	chp-chp	width of the labial philtrum	Mouth
	ch-ch	width of the mouth	Mouth
	go-go	width of the mandible	Face
Sagittal (all paired, except sn-prn)	gl-t	depth of the supraorbital rim	Upper face
	ex-t	orbitotragial distance	Upper face
	n-t	depth of the upper third of the face	Upper face
	sn-t	depth in the maxillary region	Mid face
	sn-prn	nasal tip protrusion	Nose
	gn-t	depth in the mandibular region	Lower face
	go-gn	depth of the lower jaw	Lower face
	pra-pa	ear width	Ear

Figure 2.17. Z-score values of the vertical plane distances calculated for the child with HPE and her mother. l and r indicate left and right sides of the face (study 3) [30].

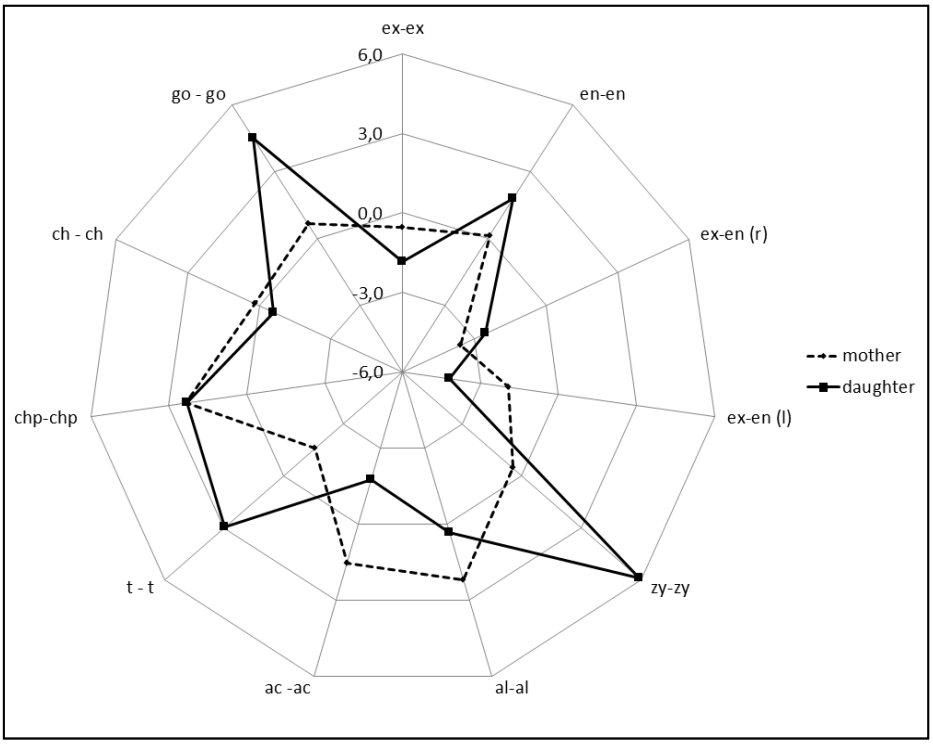

Figure 2.18. Z score values of the horizontal plane distances calculated for the child with HPE and her mother. l and r indicate left and right sides of the face (study 3) [30].

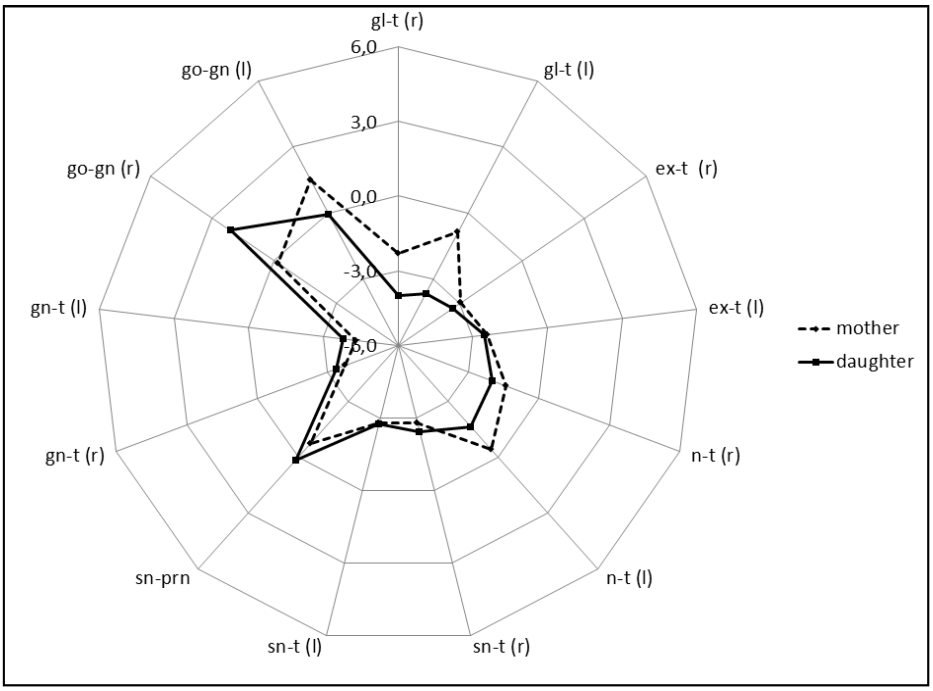

Figure 2.19. Z score values of the sagittal plane distances calculated for the child with HPE and her mother. l and r indicate left and right sides of the face (study 3) [30].

Table 2.9. Z score values that differ ± 1.5 SD from reference values in the child and her mother (study 3) [30].

Plane		Child	Mother
Vertical	tr-n	-3.7	
	tr-gn	-1.9	
	n-gn	2.3	
	n-sn		-2.3
	os-or R	4.6	
	os-or L	3.5	
	n-prn	-1.9	-2.1
	sl-gn		1.8
Horizontal	ex-ex	-1.8	
	en-en	1.8	
	ex-en R	-2.5	-1.9
	ex-en L	-4.2	-3.6
	zy-zy	5.9	
	al-al		2.2
	t-t	3	-1.6
	chp-chp	2.3	2.3
	go-go	4.5	
Sagittal	gl-t R	-4	-2.3
	gl-t L	-3.6	
	ex-t R	-3.4	-3
	ex-t L	-2.5	-2.4
	n-t R	-2	
	n-t L	-1.6	
	sn-t R	-2.4	-2.8
	sn-t L	-2.8	-2.8
	gn-t R	-3.3	-4.3
	gn-t L	-3.8	-3.7
	go-gn R	2.1	
	pra-pa R	-2.9	
	pra-pa L	-5.6	

3. FACIAL MORPHOMETRIC ANALYSIS: SURFACE-BASED APPROACH

In this section some studies, executed by means of a stereophotogrammetric analysis of the face and conducted through a surface-based approach, will be reported.

Indeed, stereophotogrammetry also allows the reconstruction of the entire facial surface, thus permitting the performance of more complex analyses, as the evaluation of the level of facial asymmetry and the study of facial mimicry, leading to big advantages for the planning, follow up and final assessment of facial surgical treatments [23].

3.1 Study 4: 3D stereophotogrammetric assessment of labial symmetry in a girl treated for a lymphatic malformation.

Lymphatic malformations (LMs) are rare and non-malignant masses containing lymph, vessels and chambers, frequently involving the head and neck, that can compress or obstruct surrounding structures, impairing facial functionality and appearance [113]. Treatment of macrocystic LMs usually consists of sclerotherapy, while microcystic LMs are treated through a gross debulking and/or camouflage procedures [114,115]. Computed tomography (CT) and magnetic resonance imaging (MRI) can help the diagnosis of the disease and assess its follow up, but these techniques are expensive, time consuming and invasive (CT in particular), thus not permitting their routine use and the performance of repeated evaluations [116,20].

In order to overtake these problems, the technological advancement has provided new solutions for the morphological analysis of the external soft tissues only [18]. Stereophotogrammetry, for example, allows the safe and fast reconstruction of facial soft tissues, therefore permitting accurate and reproducible multiple evaluations [19,22].

In this study, subsequent stereophotogrammetric evaluations of the symmetry of the labial area of a Caucasoid 16-year-old girl, affected by a microcystic lymphatic malformation and surgically treated were performed. The evaluations were executed in order to objectively assess the treatment progression and final results.

Since the multifocal diffusion of the masses and a high recurrence risks, the surgery of microcystic lymphatic malformation has always been quite challenging thus demotivating patients to be compliant to a multistage treatment [117,118]. The procedure here described permits and easy and rapid assessment of the on-going achieved results, providing objective and easy-to understand indicators, both for the clinicians and, especially, for the patients, who can be encouraged to carry on the treatment.

3.2 MATERIALS AND METHODS

The girl analysed in this study came for observation for the first time at the age of 16 years. She presented a microcystic lymphatic malformation on her right facial half, previously treated, through several partial removals in another hospital, since the age of 12. Her facial nerve was injured during one of the previous surgical sessions. The long-standing unilateral facial paralysis was treated with a free gracilis muscle transfer, innervated by homolateral masseteric nerve [119]. The residual deformity involved the right side facial soft tissues in the labial area, parasymphysis and mandibular body.

The first surgical phase consisted on the creation of a new labial commissure, by removing two myomucosal wedges at the angle of the mouth, to symmetrize its mediolateral position [120,121]. A skin flap was simultaneously made, inciding the nasolabial fold to ameliorate the vertical position of the commissure.

After 6 months, an osteotomy of the mandibular body with genioplasty was executed and 7 months after mandibular surgery, a suspension of the right cheek with fascia lata was performed [122,123].

Three stereophotogrammetric evaluations were made. The first one before the treatment to the oral commissure; the second one six months after the reconstruction of the commissure and before mandibular surgery; the last one six months after suspension with fascia lata. Figure 3.20 shows a 3D reconstruction of the patient facial skeleton, obtained from CT data, before and after the surgical procedure, while figure 3.21 shows the stereophotogrammetric facial reconstructions acquired at the same phases.

The stereophotogrammetric acquisitions were executed with the VECTRA M3 system (Canfield Scientific Inc, Fairfield, NJ, USA). Before the acquisitions, a series anatomical landmarks was visually identified, or individuated by palpation on the patient's face, through a black, biocompatible, liquid eyeliner. This procedure was performed by an expert operator and executed according to the protocol described in paragraph 1.4 [94].

The patient was asked to be seated in front of the stereophotogrammetric system, in a relaxed way, with the face in a neutral expression and teeth in loose contact. The 3D facial images were subsequently obtained.

On the 3D reconstructed facial, an off-line working protocol was applied. In particular, the anatomical landmarks were digitally identified and a subset of them was used to automatically

select a portion of face that permits the automatic detection of the midline plane of facial symmetry, excluding hair and neck. These procedures, performed through Mirror® (Canfield Scientific Inc., Fairfield, NJ), the imaging software of the VECTRA system, are described and validated in literature [23].

Once the area of interest was identified, the labial surface (LS) was manually segmented from it. The intra-operator repeatability of LS selection was tested in the facial areas of 10 reference healthy subjects, paired for sex, age and ethnic group to the patient and extracted from our database.

Since LS selection was the only manual step of the procedures and had not been previously validated, the repeatability analysis was performed only on this phase, through linear regression and Bland and Altman analysis [124].

To segment the lips, the operator delimitated the LS with an arbitrarily defined number of 70 points, starting from the landmark “labiale superius” (ls) and following the labial contour in clockwise direction, to the same landmark (Figure 3.22).

Thanks to these points, the machine software was able to automatically select the LS and remove the surrounding FA. Then the midline plane, previously selected, was used to copy and reflect the LS around it.

Subsequently, it was possible to calculate the Root Mean Square Deviation (RMSD) between the original and the reflected LS. An example of copied and reflected LS is shown in figure 3.23.

This off-line protocol was repeated for all the stereophotogrammetric acquisitions, in order to objectify the change in terms of symmetry of the LS during the different phases of the surgical treatment.

Considering the landmarks “subnasale, “cheilion” and “stomion”, a set of linear measurements was also calculated during the different treatment phases (Figure 3.24). In particular, mouth width (ch_r-ch_l) and the ch_r-sn, ch_l-sn, ch_r-sto and ch_l-sto linear distances were computed. The obtained measurements were compared with reference values from the previously selected 10 reference women, through z score calculation. Z scores were also calculated for RMSD, using reference values coming from the same group.

3.3 RESULTS

The R^2 value from the linear regression analysis for LS repeated measurements was 0.99, indicating a very high correlation between the measurements. Figure 3.25 shows the Bland-Altman plot for the same measurements. The very low bias value (-0.02 cm^2), indicated that LS was measured with almost the same values in both the repetitions; reproducibility was very high (95.9%).

RMSD evaluated during the successive phases of the surgical treatment were respectively 5.8, 2.5 and 1.7 mm. Their progressive reduction during surgical treatment corresponds to an increase in terms of labial symmetry. Values closer to 0 indicate high symmetry level, while negative or positive values indicate negative or positive deviations from the perfect symmetry condition.

Z score values for both the linear measurements and the RMSD are presented in table 3.10. During the progression of the treatment, the z scores reduced, becoming very similar to those of the reference group (that are equal to 0), and showing the successful result of the surgical interventions.

3.4 DISCUSSION AND CONCLUSIONS

Labial asymmetry can be linked to several pathological conditions, which include not only lymphatic but also different malformations, for example cleft lip and palate, macrostomia, Parry Romberg syndrome and others [125,126].

Patients' quality of life can be seriously affected by labial or facial asymmetry in general, involving functional, aesthetic, and psychological aspect. From this point of view, a quantitative assessment of the asymmetry degree is relevant [23,127].

Furthermore, the identification of morphological parameters to objectively assess labial asymmetry may be very useful from a clinical point of view: it may support surgeons and clinicians to define their therapeutic strategies and motivate the patient to carry on the therapy [125].

Three-dimensional methods have been suggested as the more appropriate techniques among all that have been proposed to assess labial asymmetry [128]. Optical systems are very fast, reliable and accurate; thanks to their safety, they allow for the repeated, longitudinal acquisition of 3D facial and therefore labial morphology, avoiding any risk for patients and operators [20,125].

Moreover the 3D approach permits the rotation of the image around all the axes, thus facilitating, for example, the segmentation of the region of interest, as the LS. This procedure, in fact, is

facilitated by the possibility of visualising the labial profile from multiple points of view. This procedure improves, moreover, the intra-operator repeatability of LS selection, compared to that performed by freehand drawing, as done by Russell et al. in two-dimensional labial images [129,130].

In the current study, facial area selection and labial segmentation are the only manual steps. Repeatability of facial area selection has already been proven [23]; for labial segmentation, the Bland and Altman analysis executed in this study confirmed the good intra-operator repeatability (with a negligible systematic error of underestimation, compared to the measurement dimension, indicated by the low bias value of -0.18%) (Figure 3.25)[124].

Furthermore, RMSD, which was used for an objective evaluation of the labial asymmetry, proved to be a good indicator, confirming existing literature [20,131,132]. Indeed, the patient here evaluated underwent an important reduction of the RMSD (and corresponding z score value), after the first surgical treatment (Table 3.10). This means a great decrease of labial asymmetry and justifies the oral commissure plastic as first treatment, even to meet the patient's compelling requirements, since the unsatisfying results obtained by the previous surgeries.

The increase of symmetry was maintained, as indicated by the additional reduction of the RMSD z scores. The same reduction was found for the z scores of the calculated linear distances.

It is not possible to obtain a perfect symmetry in biological systems, and a perfect symmetric face is not always considered attractive, however, in the case of severe impairment, social life and psychology of the affected people can be seriously compromised [133,134]. Since different conditions lead to the asymmetry of labial area, the current study offers a reliable, fast, easy and safe method for the initial evaluation and follow-up of the involved area.

Moreover, the objective results provided by the stereophotogrammetric analysis can motivate the patients to be more adherent to the therapy and more confident of medical decisions. This is particularly relevant for the treatment of facial microcystic LMs, where the anatomy is usually severely affected and where clear guidelines to symmetrise the face are not available.

3.5 Study 5: Facial reanimation assessment performed through 3D-3D superimposition: a new method.

Several causes can lead to facial palsy, including the outcome of specific surgical treatment at the cranial base and brain; thus provoking clinical and psychological problems that can severely alter patients' quality of life [135-137].

Surgical facial reanimation is currently aimed at providing a new neural stimulus and the hypoglossal and masseteric nerves are the most frequently used, partially modifying their function through a cerebral adaptation [138-140].

Their native function still provides a bigger stimulus (smiling and contemporary clenching the teeth or pushing the tongue against lower incisors), nevertheless this types of smile cannot be spontaneous, since the facial nerve only can be activated by emotions [135]. For this reason one or more branches of the contralateral unaffected facial nerve can be used to perform a "cross-face" nerve graft, trying to qualitatively ameliorate the smile, through the spontaneity [141].

Currently, the assessment of the restored facial functions is performed through traditional methods which consist of clinical classifications (e.g. House-Brackmann scale) simple to use, but qualitative and observer-dependent [136,142-144]. In order to create an gold standard assessment method, the Harward facial paralysis team proposed the e-FACE evaluation; a widely adopted method, that allow inter-centres comparisons; even if it still relies on observer evaluations [145].

The introduction of new technologies has now permitted the application of the 3D analysis of faces to facial palsy patients [136,146,147]. Nevertheless, previous studies have analysed facial mimicry limited to the movement of specific reference landmarks.

The 3D analysis of faces now permits the execution of more complex evaluations, for example through 3D facial models superimpositions and calculation of point-to-point distances between the facial surfaces [148,149]. The aim of this study is to introduce a new method for evaluating the outcome of facial reanimation surgery through a 3D-3D registration and superimposition procedure, thus providing objective and quantitative results of the surgical treatment.

3.6 MATERIALS AND METHOD

Eleven subjects, of age comprised between 42 and 77 years (mean: 58.18 years; SD: 11.44 years) and affected by unilateral facial palsy were analysed. For the majority of cases the palsy was caused by the surgical removal of an acoustic neurinoma (Table 3.11).

An interval of time comprised between 6 and 18 months had passed between facial nerve lesion and surgery, while between 13 and 43 months had passed between surgery and 3D facial analysis.

All patients underwent a one-time surgery based on triple innervation: end-to-end masseteric to temporofacial branch neurorrhaphy, side-to-end hypoglossus to cervicofacial branch neurorrhaphy and two crossface sural nerve grafts.

Before all procedures, a detailed description was provided to all patients who gave their written informed consent. The consent form had previously been approved by the ethical committee of the University of Milan Medical School, in accordance with the standards of the 1964 Declaration of Helsinki.

The procedures were safe and did not create pain or discomfort. Each patient was imaged 5 times by the stereophotogrammetric system VECTRA M3 3D® (Canfield Scientific, Inc., Fairfield, NJ). The acquisitions were performed after a landmarking procedure, as described in paragraph 1.4.

The facial models were obtained asking the patients to perform different manoevres, in particular they were asked to:

- stay in a resting position;
- smile on the healthy side, thus activating the cross-face procedure;
- clench, thus activating masseteric neurorrhaphy;
- push with the tongue against the lower incisors, thus activating hypoglossal neurorrhaphy;
- produce the most spontaneous corner-of-the-mouth smile using all the previous mentioned strategies.

The 3D smiling facial models were then superimposed on the corresponding neutral one, for a total of four superimpositions for each patient. In order to perform a precise registration, a facial area of interest (FAI) was segmented in each model [23]. The software of the stereophotogrammetric system allowed the automatic superimposition of the FAIs, executed in order to reach the least distance between corresponding points of the entire surfaces (Figure 3.26). After the registration between the couples of corresponding surfaces, the facial reconstructions were further segmented in order to divide them in two halves, according to six midline landmarks (tr, n, prn, sn, sl, pg, gn) and the point-to-point root mean square deviation

(RMSD) value between the neutral expression model and the different types of smile was automatically calculated through the Mirror Vectra software (Canfield Scientific, Inc., Fairfield, USA), taking into consideration separately the paralysed and healthy facial sides.

Moreover, an asymmetry index was calculated from RMSD values as the absolute value of the following formula: (RMSD healthy side – RMSD paralysed side)*100/ RMSD healthy side.

The same and another operator repeated all the procedures (for a total of 24 superimpositions), in order to verify intra-and-inter-operator error, which were respectively assessed through Bland-Altman test.

Results were further analysed through a two-way ANOVA, in order to ascertain statistically significant differences of RMS values according to the side, type of stimulus and their interaction. The level of significance was set at 0.05.

For both tests, post-hoc comparisons were performed separately for the affected and healthy side using a one-way ANOVA, with a level of significance corrected at $p < 0.0125$.

A one-way ANOVA was used to verify the presence of statistically significant differences according to the type of stimulus for symmetry indices. The level of significance was set at $p<0.05$, post-hoc tests were executed when necessary.

3.7 RESULTS

The intra- and interobserver repeatability of the extraction procedure of RMSD values was 97%.

Considering the unaffected facial side, cross-face stimulus and masseteric stimulus (smiling on the healthy side and biting, respectively) allowed the obtaining of the highest RMSD values.

The same parameters were lower on the paralysed side than on the unaffected one: masseteric stimulus had the highest RMSD distance in comparison to the rest position, followed by the hypoglossal one. Corner of the mouth smile reached intermediate values for both the affected and unaffected sides (Table 3.12).. Statistically significant differences were found for side (F: 23.48; P: <0.0001) and type of stimulus (F: 2.8; P: 0.0453). Side x stimulus interaction was not statistically significant (F: 2.3; P: 0.0836). Post-hoc test revealed statistically significant differences between the facial and the masseteric stimulus on the unaffected side, and between the facial and hypoglossal stimulus on the paralysed side ($p<0.0125$).

The facial cross-face stimulus contributed to the highest asymmetry index, while the masseteric stimulus induced the most symmetric movements of face. Statistically significant differences were found for the type of stimulus (F: 3.64; P: 0.0237), although post-hoc tests revealed differences only between the facial and masseteric stimuli.

3.8 DISCUSSION AND CONCLUSIONS

Facial palsy leads to functional and psychological consequences, especially connected to the asymmetry and distortion of the face; in this context, facial reanimation proved to be a surgical option for reducing facial palsy effects, nevertheless a generally agreed quantitative method for the assessment of facial movements is still lacking [135,137-138].

Although they permit inter-centres comparisons, current clinical methods are qualitative, and do not quantify the facial modifications evoked by different stimuli [146].

The introduction of modern 3D acquisition and elaboration technologies has allowed the improvement of the analyses on facial motion, as demonstrated by Popat et al. who used a stereophotogrammetric motion analyser, even if their method was limited to the analysis of some types of movements. A similar method was also used by Okada through laser scanning [150-152].

In our laboratory, we have applied a repeatable method for the quantitative assessment of facial mimicry based on the 3D displacement of landmarks detected by a motion capture system [136,153,154]. Unfortunately, this instrument is not common, and it is improbable that its use may become diffuse [155], therefore we devised the current protocol, that can be performed with any optical instrument; whose diffusion is progressively increasing.

Our results confirm literature for what concerns the surgical techniques. Indeed, cross-face intervention does not allow significant facial movements, being a “qualitative” nervous connection, while the masseteric stimulus provokes the greatest facial modifications [135]. The highest facial asymmetry is obtained by the facial cross-face stimulus, as it stimulates the movement on the healthy side, while the affected one is minimally involved; on the other side, the masseteric one provides the most symmetric expression. “Corner of the mouth smile” allowed the obtaining of intermediate levels of both facial movement and asymmetry, as after surgery patients spontaneously learned that the most “natural” smile can be obtained through a limited activation of muscles on the unaffected side, increasing the symmetry of the expression [135,136].

In conclusion, this study showed a new, highly repeatable method for the evaluation of facial movements in patients who underwent facial reanimation surgery, being useful in the follow-up evaluation and final assessment of the success of surgical treatment.

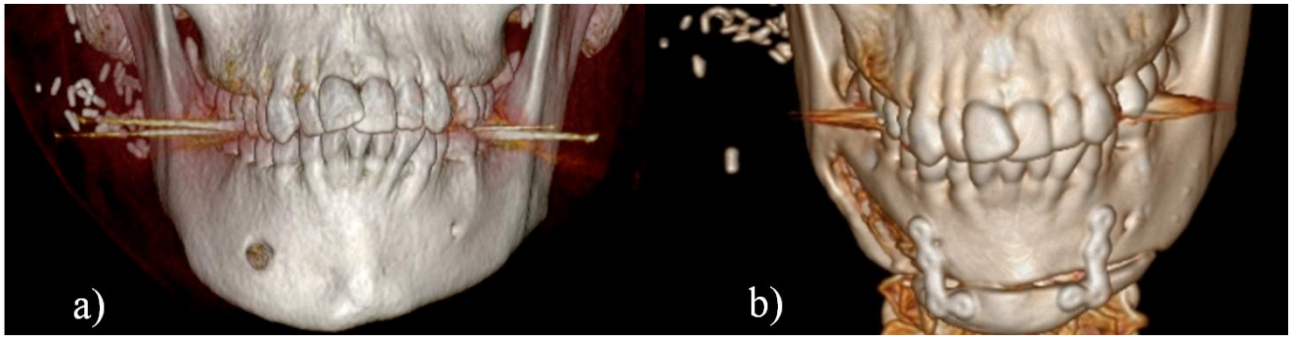

Figure 3.20. Three-dimensional CT reconstruction of the patient facial skeleton; a) before surgical treatment; b) after surgical treatment (study 4) [7].

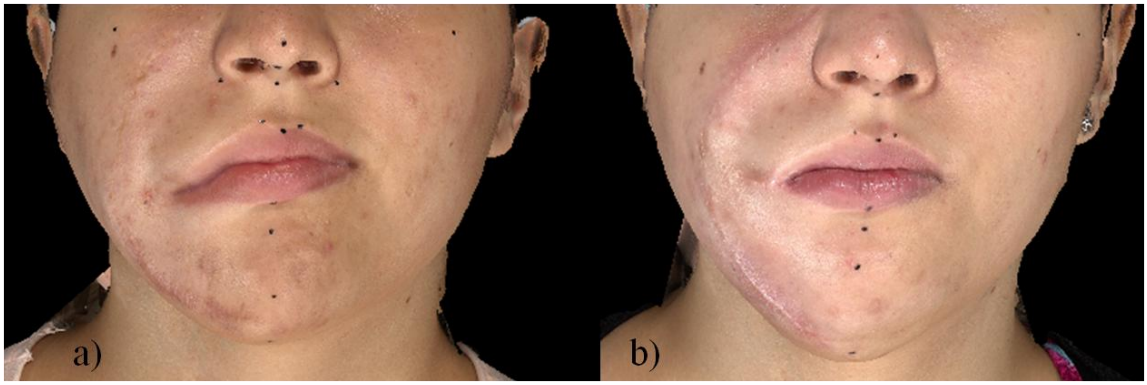

Figure 3.21. Three-dimensional stereophotogrammetric reconstruction of the patient face; a) before surgical treatment; b) after surgical treatment (study 4)[7].

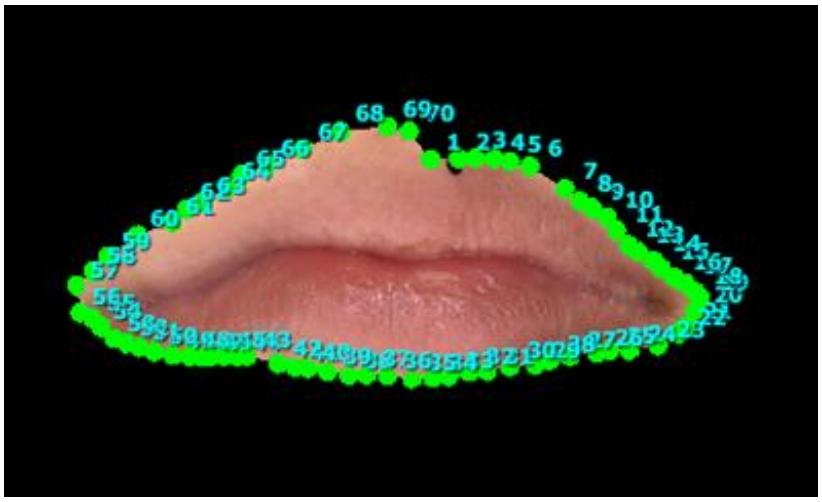

Figure 3.22. Example of labial surface segmentation [7].

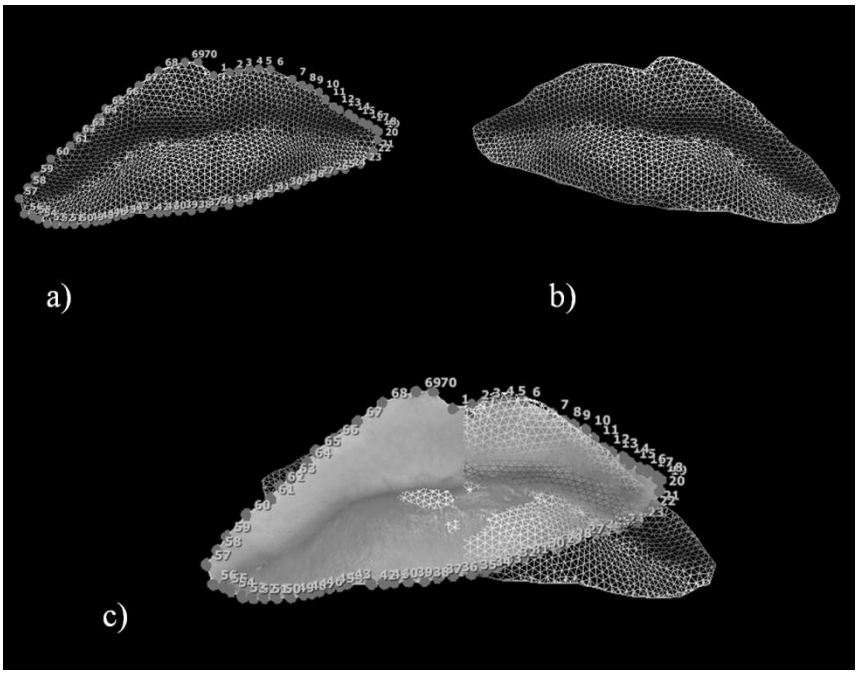

Figure 3.23. a) Example of segmented labial surface; b) labial surface copied and reflected around the Y axis; c) superimposition of the original and copied labial surfaces.

Segmented lips correspond to the pre-surgical treatment stage [7].

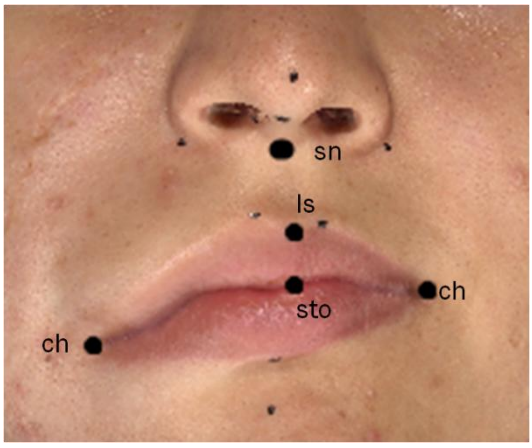

Figure 3.24. Landmarks used to calculate linear distances [7].

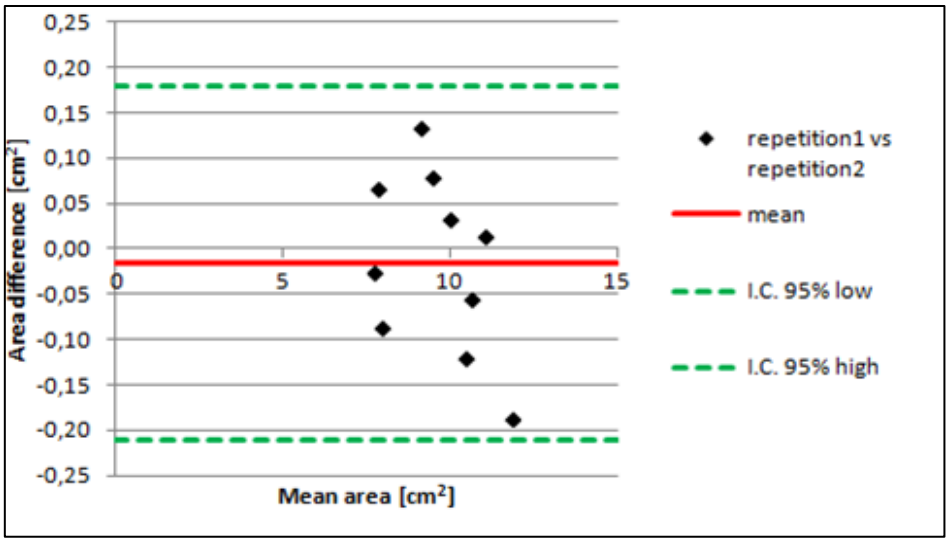

Figure 3.25. Bland and Altman plot for the repeated measurements of the labial area. Continuous line indicates the bias, dashed lines the intervals of confidence [7].

Table 3.10. Summary of the z scores values calculated during the different treatment phases for both linear measurements and RMSD. **ch** indicates the point located at the oral commissure; **sn** indicates the point located in the midline in the lowest part of the columella; **sto** indicates the point located in the midline between the lips. r and l indicate respectively the right and left facial side. Z scores of the unaffected side are also reported [7].

z-score	**Surgery #1**	**Surgery #2**	**Surgery #3**
ch-ch	2.5	1.3	0.3
ch_r-sn	5.6	2.8	0.1
ch_l-sn	1.7	1.1	0
ch_r-sto	3.5	0.6	-0.8
ch_l-sto	1.2	1.5	0.5
RMSD	10.6	3.1	1.3

Table 3.11. Clinical data of the 11 patients selected for study 5; pre-operative House-Brackmann score is six for all the patients.

Sex	**Age (years)**	**Diagnosis**	**Time period between surgery and 3D analysis (months)**	**Post-operative House-Brackmann score**
Female	66	Acoustic neurinoma	15	2
Male	49	Acoustic neurinoma	14	3
Male	69	Acoustic neurinoma	43	3
Female	52	Acoustic neurinoma	29	2
Male	59	Acoustic neurinoma	22	2
Male	76	Acoustic neurinoma	23	2
Female	53	Car accident	13	3
Female	47	Acoustic neurinoma	19	2
Female	67	Acoustic neurinoma	14	2
Female	42	Acoustic neurinoma	32	2
Female	68	Neoformation of the petrous portion of temporal bone	35	3

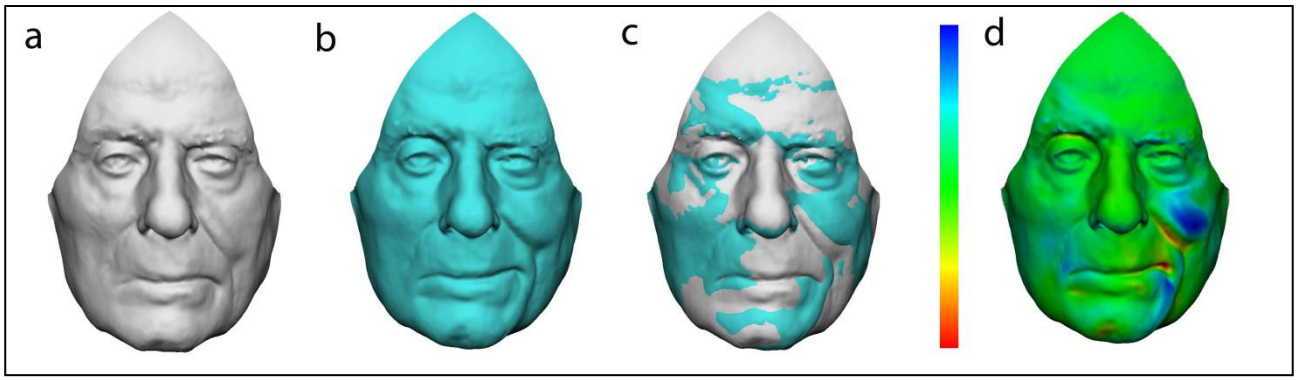

Figure 3.26. 1: steps of 3D-3D superimposition: a) 3D model of the patient in rest position; b) 3D model of the patient (corner-of-the-mouth smile); c) registration according to the least point-to-point distance between the two models; d) chromatic map of distances between the two models: in green unchanged areas, in blue areas more prominent in the smiling model than in the rest position, and vice versa for the red and yellow areas. In this case the right side is the paralysed one and shows a prevalence of green coloration.

Table 3.12. RMSD values for the healthy and paralysed sides and asymmetry index for all the four elicited stimuli. Values are mean and (standard deviation).

	Facial cross-face stimulus	**Hypoglossal stimulus**	**Masseteric stimulus**	**"Corner-of-the-mouth smile"**
Healthy side (mm)	1.38 (0.63)	0.82 (0.44)	1.31 (0.46)	1.13 (0.53)
Paralyzed side (mm)	0.54 (0.24)	0.67 (0.31)	0.95 (0.49)	0.59 (0.14)
Asymmetry index (%)	62 (28)	42 (25)	30 (22)	41 (20)

4. GENERAL CONCLUSION

In this thesis, facial morphometric analyses executed through stereophotogrammetry were performed, using both a landmark-based approach and a surface based approach for different purposes.

The aims of the different stereophotogrammetric facial assessments here presented, indeed, included:

- the identification of facial features, common among patients, to help/support the clinical diagnosis of two syndromes (Dravet and Glut-1 deficiency syndromes) whose recognition may be difficult through conventional methods, such as clinical investigations and genetic evalutations (studies 1 and 2);
- the identification of facial features common among adult patients affected by Dravet syndrome, to help the disease's recognition even in adult misdiagnosed cases (study 1);
- the better characterisation of the 3D facial traits associated to a case of holoprosencephaly and the evaluation of their possible correlation with the clinical picture (study 3);
- the quantitative assessment of the results of surgical procedures involving facial surface or facial mimicry and their follow up (studies 4 and 5).

Stereophotogrammetry proved to be an excellent tool to achieve all these objectives.

Accurate and reliable, stereophotogrammetric systems are non invasive and fast instruments, suitable for the analysis of different categories of subjects, including children and individuals with mental delay or not completely collaborative, as some of the participants in studies 1, 2 and 3. Being contactless, stereophotogrammetry does not create compression artefacts and allows the identification of objective facial parameters, helpful for both clinical assessment and increasing the treatment compliance of the subject/patient to be analysed. Therefore, their increasing use in clinical and research studies is completely justified [7,20].

Despite an initial considerable price, stereophotogrammetric systems' running costs are sufficiently low. However, nowadays, cheaper portable instruments are available and related literature sustains their accuracy for the majority of clinical applications, including the possibility to compare and/or combine acquisitions obtained from them to those acquired with the classical unmovable systems [156,157].

Nonetheless, the 3D reconstructions obtained through all, old and new systems, can be easily collected and shared among researchers and clinicians, thus creating databases and digital

archives. An example is represented by the “FaceBase Hub Data Repository” a digital archive, financed by the National Institute of Health (NIH) and aimed at collecting as much as possible facial reconstructions, to better define the craniofacial alterations associated to genetic syndromes, through a computerised facial-analysis system [158].

Technology will never substitute persons, and in the current context computerised evaluations should be considered as a support to clinical assessments, facilitating diagnosis and providing suggestions for a better treatment.

REFERENCES

[1] Dion K, Berscheid E, Walster E. What is beautiful is good. J Pers Soc Psychol. 1972;24(3):285-290.

[2] https://www.omim.org/entry/190685, accessed on August 11 2017.

[3] Sforza C, Elamin F, Dellavia C, Rosati R, Lodetti G, Mapelli A, Ferrario VF. Morphometry of the orbital region soft tissues in Down syndrome. J Craniofac Surg. 2012;23(1):198-202.

[4] Farkas LG. Anthropometry of the head and face. Raven Press 1994.

[5] Spencer F. History of physical anthropology: an encyclopedia. Garland Pub., New York, 1997.

[6] Dolci C, Pucciarelli V, Codari M, Gibelli D, Marelli S, Trifirò G, Pini A, Sforza C. 3D Craniofacial Morphometric Analysis of Young Subjects with Marfan Syndrome: A Preliminary Report. Proceedings of the 6th International Conference on 3D Body Scanning Technologies, Lugano, Switzerland, 27-28 October 2015.

[7] Pucciarelli V, Tarabbia F, Codari M, Guidugli GA, Colletti G, Dell'Aversana Orabona G, Bianchi B, Sforza C, Biglioli F. Stereophotogrammetric Evaluation of Labial Symmetry After Surgical Treatment of a Lymphatic Malformation. J Craniofac Surg. 2017;28(4):e355-e358.

[8] Sforza C, Grandi G, Binelli M, Dolci C, De Menezes M, Ferrario VF. Age- and sex-related changes in three-dimensional lip morphology. Forensic Sci Int. 2010;200(1-3):182.e1-7.

[9] Sforza C, Grandi G, Binelli M, Tommasi DG, Rosati R, Ferrario VF. Age- and sex-related changes in the normal human ear. Forensic Sci Int. 2009;187(1-3):110.e1-7.

[10] Ferrario VF, Sforza C, Poggio CE, Cova M, Tartaglia G. Preliminary evaluation of an electromagnetic three-dimensional digitizer in facial anthropometry. Cleft Palate Craniofac J. 1998;35(1):9-15.

[11] Ferrario VF, Dellavia C, Zanotti G, Sforza C. Soft tissue facial anthropometry in Down syndrome subjects. J Craniofac Surg. 2004;15(3):528-532.

[12] Sforza C, Ferrario VF. Soft-tissue facial anthropometry in three dimensions: from anatomical landmarks to digital morphology in research, clinics and forensic anthropology. J Anthropol Sci. 2006;84:97-124.

[13] Ferrario VF, Dellavia C, Serrao G, Sforza C. Soft tissue facial angles in Down's syndrome subjects: a three-dimensional non-invasive study. Eur J Orthod. 2005;27(4):355-362.

[14] Benington PC, Gardener JE, Hunt NP. Masseter muscle volume measured using ultrasonography and its relationship with facial morphology. Eur J Orthod. 1999;21(6):659-670.

[15] Zhou J, Espinoza Orías AA, Kang X, He J, Zhang Z, Inoue N, An HS. CT-based morphometric analysis of the occipital condyle: focus on occipital condyle screw insertion. J Neurosurg Spine. 2016;25(5):572-579.

[16] Sholts SB, Wärmländer SK, Flores LM, Miller KW, Walker PL. Variation in the measurement of cranial volume and surface area using 3D laser scanning technology. J Forensic Sci. 2010;55(4):871-876.

[17] Kovacs L, Zimmermann A, Brockmann G, Gühring M, Baurecht H, Papadopulos NA, Schwenzer-Zimmerer K, Sader R, Biemer E, Zeilhofer HF. Three-dimensional recording of the human face with a 3D laser scanner. J Plast Reconstr Aesthet Surg. 2006;59(11):1193-1202.

[18] Kovacs L, Zimmermann A, Brockmann G, Baurecht H, Schwenzer-Zimmerer K, Papadopulos NA, Papadopoulos MA, Sader R, Biemer E, Zeilhofer HF. Accuracy and precision of the three-dimensional assessment of the facial surface using a 3-D laser scanner. IEEE Trans Med Imaging. 2006;25(6):742-754.

[19] Codari M, Pucciarelli V, Pisoni L, Sforza C. Laser scanner compared with stereophotogrammetry for measurements of area on nasal plaster casts. Br J Oral Maxillofac Surg. 2015;53(8):769-770.

[20] Sforza C, de Menezes M, Ferrario V. Soft- and hard-tissue facial anthropometry in three dimensions: what's new. J Anthropol Sci. 2013;91:159-184.

[21] www.canfieldsci.com, accessed on August 11 2017.

[22] Sforza C, De Menezes M, Bresciani E, Cerón-Zapata AM, López-Palacio AM, Rodriguez-Ardila MJ, Berrio-Gutiérrez LM. Evaluation of a 3D stereophotogrammetric technique to measure the stone casts of patients with unilateral cleft lip and palate. Cleft Palate Craniofac J. 2012;49(4):477-483.

[23] Codari M, Pucciarelli V, Stangoni F, Zago M, Tarabbia F, Biglioli F, Sforza C. Facial thirds-based evaluation of facial asymmetry using stereophotogrammetric devices: Application to facial palsy subjects. J Craniomaxillofac Surg. 2017;45(1):76-81.

[24] Farkas LG. Anthropometry of the Head and Face. New York: Raven Press; 1994:58.

[25] Farkas LG. Anthropometry of the Head and Face. New York: Raven Press; 1994:20-25.

[26] Ferrario VF, Sforza C, Serrao G, Ciusa V, Dellavia C. Growth and aging of facial soft tissues: A computerized three-dimensional mesh diagram analysis. Clin Anat. 2003;16(5):420-433.

[27] Dolci C, Pucciarelli V, Codari M, Marelli S, Trifirò G, Pini A, Sforza C. 3D Morphometric Evaluation of Craniofacial Features in Adult Subjects with Marfan Syndrome. Proceedings of the 7th International Conference on 3D Body Scanning Technologies, Lugano, Switzerland, 30 Nov.-1 Dec. 2016.

[28] Pucciarelli V, Codari M, Invernizzi C, Bertoli S, Battezzati A, De Amicis R, De Giorgis V, Veggiotti P, Sforza C. Three-Dimensional Craniofacial Features of Glut1 Deficiency Syndrome Patients. 6th International Conference on 3D Body Scanning Technologies, Lugano, Switzerland, 27-28 October 2015.

[29] Kjaer I. Human prenatal craniofacial development related to brain development under normal and pathologic conditions. Acta Odontol Scand. 1995;53(3):135-143.

[30] Pucciarelli V, Bertoli S, Codari M, Veggiotti P, Battezzati A, Sforza C. Facial Evaluation in Holoprosencephaly. J Craniofac Surg. 2017;28(1):e22-e28.

[31] De Menezes M. Three-dimensional facial anthropometry. PhD thesis, December 20^{th,} 2010.

[32] Pucciarelli V, Bertoli S, Codari M, De Amicis R, De Giorgis V, Battezzati A, Veggiotti P, Sforza C. The face of Glut1-DS patients: A 3D Craniofacial Morphometric Analysis. Clin Anat. 2017;30(5):644-652.

[33] Dravet C. Les épilepsies graves de l'enfant. Vie Méd. 1978;8: 543-548.

[34] Dravet C, Bureau M, Dalla Bernardina B, Guerrini R. Severe myoclonic epilepsy in infancy (Dravet syndrome) 30 years later. Epilepsia. 2011; 52 Suppl 2:1-2.

[35] Claes L, Del-Favero J, Ceulemans B, Lagae L, Van Broeckhoven C, De Jonghe P. De novo mutations in the sodium-channel gene SCN1A cause severe myoclonic epilepsy of infancy. Am J Hum Genet. 2001;68(6):1327-1332.

[36] Marini C, Scheffer IE, Nabbout R, Suls A, De Jonghe P, Zara F, Guerrini R. The genetics of Dravet syndrome. Epilepsia. 2011;52 Suppl 2:24-29.

[37] Vadlamudi L, Dibbens LM, Lawrence KM, Iona X, McMahon JM, Murrell W, Mackay-Sim A, Scheffer IE, Berkovic SF. Timing of de novo mutagenesis--a twin study of sodium-channel mutations. N Engl J Med. 2010;363(14):1335-1340.

[38] Singh R, Andermann E, Whitehouse WP, Harvey AS, Keene DL, Seni MH, Crossland KM, Andermann F, Berkovic SF, Scheffer IE. Severe myoclonic epilepsy of infancy: extended spectrum of GEFS+? Epilepsia. 2001;42(7):837-844.

[39] Sugawara T, Mazaki-Miyazaki E, Fukushima K, Shimomura J, Fujiwara T, Hamano S, Inoue Y, Yamakawa K. Frequent mutations of SCN1A in severe myoclonic epilepsy in infancy. Neurology. 2002;58(7):1122-1224.

[40] Harkin LA, McMahon JM, Iona X, Dibbens L, Pelekanos JT, Zuberi SM, Sadleir LG, Andermann E, Gill D, Farrell K, Connolly M, Stanley T, Harbord M, Andermann F, Wang J, Batish SD, Jones JG, Seltzer WK, Gardner A; Infantile Epileptic Encephalopathy Referral Consortium, Sutherland G, Berkovic SF, Mulley JC, Scheffer IE. The spectrum of SCN1A-related infantile epileptic encephalopathies. Brain. 2007;130(Pt 3):843-852.

[41] Chieffo D, Ricci D, Baranello G, Martinelli D, Veredice C, Lettori D, Battaglia D, Dravet C, Mercuri E, Guzzetta F. Early development in Dravet syndrome; visual function impairment precedes cognitive decline. Epilepsy Res. 2011;93(1):73-79.

[42] Chieffo D, Battaglia D, Lucibello S, Gambardella ML, Moriconi F, Ferrantini G, Leo G, Dravet C, Mercuri E, Guzzetta F. Disorders of early language development in Dravet syndrome. Epilepsy Behav. 2016;54:30-33.

[43] Ragona F, Brazzo D, De Giorgi I, Morbi M, Freri E, Teutonico F, Gennaro E, Zara F, Binelli S, Veggiotti P, Granata T. Dravet syndrome: early clinical manifestations and cognitive outcome in 37 Italian patients. Brain Dev. 2010;32(1):71-77.

[44] Ragona F, Granata T, Dalla Bernardina B, Offredi F, Darra F, Battaglia D, Morbi M, Brazzo D, Cappelletti S, Chieffo D, De Giorgi I, Fontana E, Freri E, Marini C, Toraldo A, Specchio N, Veggiotti P, Vigevano F, Guerrini R, Guzzetta F, Dravet C. Cognitive development in Dravet syndrome: a retrospective, multicenter study of 26 patients. Epilepsia. 2011;52(2):386-392.

[45] Dravet C, Oguni H. Dravet syndrome (Severe epilepsy of the infancy)Handb Clin Neurol. 2013, 111:627-633.

[46] Dlouhy BJ, Miller B, Jeong A, Bertrand ME, Limbrick DD Jr, Smyth MD. Palliative epilepsy surgery in Dravet syndrome-case series and review of the literature. Childs Nerv Syst. 2016;32(9):1703-1708.

[47] Dutton SB, Sawyer NT, Kalume F, Jumbo-Lucioni P, Borges K, Catterall WA, Escayg A. Protective effect of the ketogenic diet in Scn1a mutant mice. Epilepsia. 2011;52(11):2050-2056.

[48] Caraballo RH, Cersósimo RO, Sakr D, Cresta A, Escobal N, Fejerman N. Ketogenic diet in patients with Dravet syndrome. Epilepsia. 2005;46(9):1539-1544.

[49] Selmer KK, Eriksson AS, Brandal K, Egeland T, Tallaksen C, Undlien DE. Parental SCN1A mutation mosaicism in familial Dravet syndrome. Clin Genet. 2009;76(4):398-403.

[50] Jansen FE, Sadleir LG, Harkin LA, Vadlamudi L, McMahon JM, Mulley JC, Scheffer IE, Berkovic SF. Severe myoclonic epilepsy of infancy (Dravet syndrome): recognition and diagnosis in adults. Neurology. 2006;67(12):2224-2226.

[51] Catarino CB, Liu JY, Liagkouras I, Gibbons VS, Labrum RW, Ellis R, Woodward C,Davis MB, Smith SJ, Cross JH, Appleton RE, Yendle SC, McMahon JM, Bellows ST, Jacques TS, Zuberi SM, Koepp MJ, Martinian L, Scheffer IE, Thom M, Sisodiya SM. Dravet syndrome as epileptic encephalopathy: evidence from long-term course and neuropathology. Brain. 2011;134(Pt 10):2982-3010.

[52] Nolan KJ, Kay E, Camfield CS, Camfield PR. Does Dravet syndrome have a recognizable face? Pediatr Neurol. 2011;45(6):392-394.

[53] De Vivo DC, Trifiletti RR, Jacobson RI, Ronen GM, Behmand RA, Harik SI. Defective glucose transport across the blood-brain barrier as a cause of persistent hypoglycorrhachia, seizures, and developmental delay. N Engl J Med. 1991;325(10):703-709.

[54] Brockmann K, Wang D, Korenke CG, von Moers A, Ho YY, Pascual JM, Kuang K, Yang H, Ma L, Kranz-Eble P, Fischbarg J, Hanefeld F, De Vivo DC. Autosomal dominant glut-1 deficiency syndrome and familial epilepsy. Ann Neurol. 2001;50(4):476-485.

[55] Klepper J. GLUT1 deficiency syndrome and ketogenic diet therapies: missing rare but treatable diseases? Dev Med Child Neurol. 2015;57(10):896-897.

[56] De Giorgis V, Varesio C, Baldassari C, Piazza E, Olivotto S, Macasaet J, Balottin U, Veggiotti P. Atypical Manifestations in Glut1 Deficiency Syndrome. J Child Neurol. 2016;31(9):1174-1180.

[57] De Giorgis V, Teutonico F, Cereda C, Balottin U, Bianchi M, Giordano L, Olivotto S, Ragona F, Tagliabue A, Zorzi G, Nardocci N, Veggiotti P. Sporadic and familial glut1ds Italian patients: A wide clinical variability. Seizure. 2015;24:28-32.

[58] Leen WG, Klepper J, Verbeek MM, Leferink M, Hofste T, van Engelen BG, Wevers RA, Arthur T, Bahi-Buisson N, Ballhausen D, Bekhof J, van Bogaert P, Carrilho I, Chabrol B, Champion MP, Coldwell J, Clayton P, Donner E, Evangeliou A, Ebinger F, Farrell K, Forsyth RJ, de Goede CG, Gross S, Grunewald S, Holthausen H, Jayawant S, Lachlan K, Laugel V, Leppig K, Lim MJ, Mancini G, Marina AD, Martorell L, McMenamin J, Meuwissen ME, Mundy H, Nilsson NO, Panzer A, Poll-The BT, Rauscher C, Rouselle CM, Sandvig I, Scheffner T, Sheridan E, Simpson N, Sykora P, Tomlinson R, Trounce J, Webb D, Weschke B, Scheffer H, Willemsen MA. Glucose transporter-1 deficiency syndrome: the expanding clinical and genetic spectrum of a treatable disorder. Brain. 2010;133(Pt 3):655-670.

[59] De Vivo DC, Leary L, Wang D. Glucose transporter 1 deficiency syndrome and other glycolytic defects. J Child Neurol. 2002;17 Suppl 3:3S15-23.

[60] Klepper J, Flörcken A, Fischbarg J, Voit T. Effects of anticonvulsants on GLUT1-mediated glucose transport in GLUT1 deficiency syndrome in vitro. Eur J Pediatr. 2003;162(2):84-89.

[61] Ramm-Pettersen A, Nakken KO, Skogseid IM, Randby H, Skei EB, Bindoff LA, Selmer KK. Good outcome in patients with early dietary treatment of GLUT-1 deficiency syndrome: results from a retrospective Norwegian study. Dev Med Child Neurol. 2013;55(5):440-447.

[62] Klepper J, Leiendecker B, Bredahl R, Athanassopoulos S, Heinen F, Gertsen E, Flörcken A, Metz A, Voit T. Introduction of a ketogenic diet in young infants. J Inherit Metab Dis. 2002;25(6):449-460.

[63] De Giorgis V, Veggiotti P. GLUT1 deficiency syndrome 2013: current state of the art. Seizure. 2013;22(10):803-811.

[64] Goodwin AF, Larson JR, Jones KB, Liberton DK, Landan M, Wang Z, Boekelheide A, Langham M, Mushegyan V, Oberoi S, Brao R, Wen T, Johnson R, Huttner K, Grange DK, Spritz RA, Hallgrímsson B, Jheon AH, Klein OD. Craniofacial morphometric analysisof individuals with X-linked hypohidrotic ectodermal dysplasia. Mol Genet Genomic Med. 2014;2(5):422-429.

[65] Leiser Y, Barak M, Ghantous Y, Yehudai N, Abu El-Naaj I. Indications for Elective Tracheostomy in Reconstructive Surgery in Patients With Oral Cancer. J Craniofac Surg. 2017;28(1):e18-e22.

[66] Zelditch ML, Swiderski DL, Sheets DH, Fink WL. 2012. Geometric morphometrics for biologists: A primer. Elsevier Academic Press, San Diego.

[67] Diomedi M, Gan-Or Z, Placidi F, Dion PA, Szuto A, Bengala M, Rouleau GA, Gigli GL. A 23 years follow-up study identifies GLUT1 deficiency syndrome initially diagnosed as complicated hereditary spastic paraplegia. Eur J Med Genet. 2016;59(11):564-568.

[68] Akman CI, Yu J, Alter A, Engelstad K, De Vivo DC. Diagnosing Glucose Transporter 1 Deficiency at Initial Presentation Facilitates Early Treatment. J Pediatr. 2016;171:220-226.

[69] Chitkara U, Lee L, Oehlert JW, Bloch DA, Holbrook RH Jr, El-Sayed YY, Druzin ML. Fetal ear length measurement: a useful predictor of aneuploidy? Ultrasound Obstet Gynecol. 2002;19(2):131-135.

[70] Jensen PJ, Gitlin JD, Carayannopoulos MO. GLUT1 deficiency links nutrient availability and apoptosis during embryonic development. J Biol Chem. 2006;281(19):13382-13387.

[71] Petryk A, Graf D, Marcucio R. Holoprosencephaly: signaling interactions between the brain and the face, the environment and the genes, and the phenotypic variability in animal models and humans. Wiley Interdiscip Rev Dev Biol. 2015;4(1):17-32.

[72] GH Sperber. Early orofacial development 2001. In: Sperber GH, editor. Craniofacial Development. Hamilton: BC Decker Inc:31–48.

[73] Ikuno K, Kajii TS, Oka A, Inoko H, Ishikawa H, Iida J. Microsatellite genome-wide association study for mandibular prognathism. Am J Orthod Dentofacial Orthop. 2014;145(6):757-762.

[74] Tassopoulou-Fishell M, Deeley K, Harvey EM, Sciote J, Vieira AR. Genetic variation in myosin 1H contributes to mandibular prognathism. Am J Orthod Dentofacial Orthop. 2012;141(1):51-59.

[75] Chen F, Li Q, Gu M, Li X, Yu J, Zhang YB. Identification of a Mutation in FGF23 Involved in Mandibular Prognathism. Sci Rep. 2015;5:11250.

[76] Kau CH, Richmond S, Zhurov A, Ovsenik M, Tawfik W, Borbely P, English JD. Use of 3-dimensional surface acquisition to study facial morphology in 5 populations. Am J Orthod Dentofacial Orthop. 2010;137(4 Suppl):S56.e1-9; discussion S56-57.

[77] http://www.omim.org/entry/236100, accessed on november 14, 2015.

[78] Cohen MM Jr. Holoprosencephaly: clinical, anatomic, and molecular dimensions. Birth Defects Res A Clin Mol Teratol. 2006;76(9):658-673.

[79] Lazaro L, Dubourg C, Pasquier L, Le Duff F, Blayau M, Durou MR, de la Pintière AT, Aguilella C, David V, Odent S. Phenotypic and molecular variability of the holoprosencephalic spectrum. Am J Med Genet A. 2004;129A(1):21-24.

[80] Winter TC, Kennedy AM, Woodward PJ. Holoprosencephaly: a survey of the entity, with embryology and fetal imaging. Radiographics. 2015;35(1):275-290.

[81] Rajesh D, Hurvi HD. How can we prevent birth of fetus with holoprosencephaly? anatomical and embryological aspects of holoprosencephaly. Natl J Integr Res Med. 2011;2:56-59.

[82] Kruszka P, Hart RA, Hadley DW, Muenke M, Habal MB. Expanding the phenotypic expression of Sonic Hedgehog mutations beyond holoprosencephaly. J Craniofac Surg. 2015;26(1):3-5.

[83] Gawrych E, Janiszewska-Olszowska J, Walecka A, Syryńska M, Chojnacka H. Lobar holoprosencephaly with a median cleft: case report. Cleft Palate Craniofac J. 2009;46(5):549-554.

[84] Kjaer I, Keeling JW, Graem N. The midline craniofacial skeleton in holoprosencephalic fetuses. J Med Genet. 1991;28(12):846-855.

[85] Kjær I. Neuro-osteology. Crit Rev Oral Biol Med. 1998;9:224–244.

[86] Nanni L, Croen LA, Lammer EJ, Muenke M. Holoprosencephaly: molecular study of a California population. Am J Med Genet. 2000;90(4):315-319.

[87] Redlinger-Grosse K, Bernhardt BA, Berg K, Muenke M, Biesecker BB. The decision to continue: the experiences and needs of parents who receive a prenatal diagnosis of holoprosencephaly. Am J Med Genet. 2002;112(4):369-378.

[88] Johnson CY, Rasmussen SA. Non-genetic risk factors for holoprosencephaly. Am J Med Genet C Semin Med Genet. 2010;154C(1):73-85.

[89] Griffiths PD, Jarvis D. In Utero MR Imaging of Fetal Holoprosencephaly: A Structured Approach to Diagnosis and Classification. AJNR Am J Neuroradiol. 2016;37(3):536-543.

[90] Genç M, Genç B, Solak A, Alkiliç L, Uyar M. Alobar holoprosencephaly, proboscis and cyclopia in a chromosomally normal fetus: Prenatal diagnosis and fetal outcome. Ital J Anat Embryol. 2015;120(2):83-88.

[91] Arangio P, Manganaro L, Pacifici A, Basile E, Cascone P. Importance of fetal MRI in evaluation of craniofacial deformities. J Craniofac Surg. 2013;24(3):773-776.

[92] Barkovich AJ. Magnetic resonance imaging: role in the understanding of cerebral malformations. Brain Dev. 2002;24(1):2-12.

[93] Malinger G, Lev D, Kidron D, Heredia F, Hershkovitz R, Lerman-Sagie T. Differential diagnosis in fetuses with absent septum pellucidum. Ultrasound Obstet Gynecol. 2005;25(1):42-49.

[94] De Menezes M, Rosati R, Ferrario VF, Sforza C. Accuracy and reproducibility of a 3-dimensional stereophotogrammetric imaging system. J Oral Maxillofac Surg. 2010;68(9):2129-2135.

[95] Saunders ES, Shortland D, Dunn PM. What is the incidence of holoprosencephaly? J Med Genet. 1984;21(1):21-26.

[96] Garn SM, Smith BH, LaVelle M. Applications of pattern profile analysis to malformations of the head and face. Radiology. 1984;150(3):683-690.

[97] Wenghoefer M, Ettema AM, Sina F, Geipel A, Kuijpers-Jagtman AM, Hansmann H, Borstlap WA, Bergé S. Prenatal ultrasound diagnosis in 51 cases of holoprosencephaly: craniofacial anatomy, associated malformations, and genetics. Cleft Palate Craniofac J. 2010;47(1):15-21.

[98] De Myer W, Zeman W, Gardella Palmer C. The face predicts the brain: diagnostic significance of medial facial anomalies for holoprosencephaly (arhinencephaly). Pediatrics 1964;34:256-263.

[99] Sperber GH. Early Orofacial Development. In Sperber GH ed. Craniofacial Development. Hamilton: BC Decker Inc, 2001:31-48.

[100] Petryk A, Graf D, Marcucio R. Holoprosencephaly: signaling interactions between the brain and the face, the environment and the genes, and the phenotypic variability in animal models and humans. Wiley Interdiscip Rev Dev Biol. 2015;4(1):17-32.

[101] Roelfsema NM, Hop WC, van Adrichem LN, Wladimiroff JW. Craniofacial variability index in utero: a three-dimensional ultrasound study. Ultrasound Obstet Gynecol. 2007;29(3):258-264.

[102] Ronen GM, Andrews WL. Holoprosencephaly as a possible embryonic alcohol effect. Am J Med Genet. 1991;40(2):151-154.

[103] Chuang L, Kuo PL, Yang HB, Chien CH, Chen PY, Chang CH, Chang FM. Prenatal diagnosis of holoprosencephaly in two fetuses with der (7)t(1;7)(q32;q32)pat inherited from the father with double translocations. Prenat Diagn. 2003;23(2):134-137.

[104] Sandal G, Tok L, Ormeci AR. A new case of holoprosencephaly-polydactyly syndrome with alobar holoprosencephaly, preaxial polydactyly and congenital glaucoma. Genet Couns. 2014;25(1):49-52.

[105] Zhang J, Yang T, Wang X, Yu H. Successful management of discordant alobar holoprosencephaly in monochorionic diamniotic twins with normal karyotype: a case report. Clin Exp Obstet Gynecol. 2015;42(1):114-116.

[106] Corcuera-Flores JR, Casttellanos-Cosano L, Torres-Lagares D, Serrera-Figallo MÁ, Rodríguez-Caballero Á, Machuca-Portillo G. A systematic review of the oral and craniofacial manifestations of cri du chat syndrome. Clin Anat. 2016;29(5):555-560.

[107] Helin H, van der Walt J, Holder M, George S. Case Report: Congenital Erythroleukemia in a Premature Infant with Dysmorphic Features. Pediatr Dev Pathol. 2016;19(4):334-337.

[108] Hong M, Krauss RS. Cdon mutation and fetal ethanol exposure synergize to produce midline signaling defects and holoprosencephaly spectrum disorders in mice. PLoS Genet. 2012;8(10):e1002999.

[109] Aoto K, Shikata Y, Higashiyama D, Shiota K, Motoyama J. Fetal ethanol exposure activates protein kinase A and impairs Shh expression in prechordal mesendoderm cells in the pathogenesis of holoprosencephaly. Birth Defects Res A Clin Mol Teratol. 2008;82(4):224-231.

[110] Marcucio R, Hallgrimsson B, Young NM. Facial morphogenesis: physical and molecular interactions between the brain and the face. In Chai Y ed. Craniofacial development Waltham: Academic Press, 2015: 308-311.

[111] Hennessy RJ, Baldwin PA, Browne DJ, Kinsella A, Waddington JL. Frontonasal dysmorphology in bipolar disorder by 3D laser surface imaging and geometric morphometrics: comparisons with schizophrenia. Schizophr Res. 2010;122(1-3):63-71.

[112] Pucciarelli V, Piazza E, Ragona F, Gibelli D, Granata T, Dolci C, Sforza C. Three-Dimensional Stereophotogrammetric Analysis of Adults Affected by Dravet Syndrome. Proceedings of 3DBODY.TECH 2017 8th International Conference and Exhibition on 3D Body Scanning and Processing Technologies, Montreal, Canada, 11-12 Oct. 2017

[113] Lerat J, Mounayer C, Scomparin A, Orsel S, Bessede JP, Aubry K. Head and neck lymphatic malformation and treatment: Clinical study of 23 cases. Eur Ann Otorhinolaryngol Head Neck Dis. 2016;133(6):393-396.

[114] Stillo F, Baraldini V, Dalmonte P, El Hachem M, Mattassi R, Vercellio G, Amato B, Bellini C, Bergui M, Bianchini G, Diociaiuti A, Campisi C, Gandolfo C, Gelmetti C, Moneghini L, Monti L, Magri C, Neri I, Paoloantonio G, Patrizi A, Rollo M, Santecchia L, Vaghi M, Vercellino N; Italian Society for the study of Vascular Anomalies (SISAV). Vascular Anomalies Guidelines by the Italian Society for the study of Vascular Anomalies (SISAV). Int Angiol. 2015;34(2 Suppl 1):1-45.

[115] Colletti G, Valassina D, Bertossi D, Melchiorre F, Vercellio G, Brusati R. Contemporary management of vascular malformations. J Oral Maxillofac Surg. 2014;72(3):510-528.

[116] Ginat DT, Robson CD. CT and MRI of congenital nasal lesions in syndromic conditions. Pediatr Radiol. 2015;45(7):1056-1065.

[117] Khunger N. Lymphatic malformations: current status. J Cutan Aesthet Surg. 2010;3(3):137-138.

[118] Elluru RG, Balakrishnan K, Padua HM. Lymphatic malformations: diagnosis and management. Semin Pediatr Surg. 2014;23(4):178-85.

[119] Biglioli F, Colombo V, Tarabbia F, Autelitano L, Rabbiosi D, Colletti G, Giovanditto F, Battista V, Frigerio A. Recovery of emotional smiling function in free-flap facial reanimation. J Oral Maxillofac Surg. 2012;70(10):2413-2418.

[120] Yoshimura Y, Nakajima T, Nakanishi Y. Simple line closure for macrostomia repair. Br J Plast Surg. 1992;45(8):604-605.

[121] Hikosaka M, Nakajima T, Ogata H, Miyamoto J. Refined simple line closure for macrostomia repair: designing a mucosal triangular flap on the commissure region. J Craniomaxillofac Surg. 2009;37(6):341-343.

[122] Lemound J, Stoetzer M, Kokemüller H, Schumann P, Gellrich NC. Modified technique for rehabilitation of facial paralysis using autogenous fascia lata grafts. J Oral Maxillofac Surg. 2015;73(1):176-183.

[123] Bianchi B, Ferri A, Ferrari S, Leporati M, Ferri T, Sesenna E. Ancillary procedures in facial animation surgery. J Oral Maxillofac Surg. 2014;72(12):2582-2590.

[124] Bland JM, Altman DG. Statistical methods for assessing agreement between two methods of clinical measurement. Lancet 1986;327:307–310.

[125] Kargl S, Malek M, Pumberger W. A newborn with esophageal atresia and a large , asymmetric mouth. Int J Pediatr Otorhinolaryngol 2015;10:84–86.

[126] McKearney RM, Williams JV, Mercer NS. Quantitative computer-based assessment of lip symmetry following cleft lip repair. Cleft Palate Craniofac J. 2013;50(2):138-143.

[127] Berlin NF, Berssenbrügge P, Runte C, Wermker K, Jung S, Kleinheinz J, Dirksen D. Quantification of facial asymmetry by 2D analysis - A comparison of recent approaches. J Craniomaxillofac Surg. 2014;42(3):265-271.

[128] Al-Omari I, Millett DT, Ayoub AF. Methods of assessment of cleft-related facial deformity: a review. Cleft Palate Craniofac J. 2005;42(2):145-156.

[129] Lekakis G, Claes P, Hamilton GS 3rd, Hellings PW. Three-Dimensional Surface Imaging and the Continuous Evolution of Preoperative and Postoperative Assessment in Rhinoplasty. Facial Plast Surg. 2016;32(1):88-94.

[130] Russell JH, Kiddy HC, Mercer NS. The use of SymNose for quantitative assessment of lip symmetry following repair of complete bilateral cleft lip and palate. J Craniomaxillofac Surg. 2014;42(5):454-459.

[131] Taylor HO, Morrison CS, Linden O, Phillips B, Chang J, Byrne ME, Sullivan SR, Forrest CR. Quantitative facial asymmetry: using three-dimensional photogrammetry to measure baseline facial surface symmetry. J Craniofac Surg. 2014;25(1):124-128.

[132] Djordjevic J, Toma AM, Zhurov AI, Richmond S. Three-dimensional quantification of facial symmetry in adolescents using laser surface scanning. Eur J Orthod. 2014;36(2):125-132.

[133] Stefanovic N, El H, Chenin DL, Glisic B, Palomo JM. Three-dimensional pharyngeal airway changes in orthodontic patients treated with and without extractions. Orthod Craniofac Res. 2013;16(2):87-96.

[134] Springer IN, Wannicke B, Warnke PH, Zernial O, Wiltfang J, Russo PA, Terheyden H, Reinhardt A, Wolfart S. Facial attractiveness: visual impact of symmetry increases significantly towards the midline. Ann Plast Surg. 2007;59(2):156-162.

[135] Biglioli F. Facial reanimations: part I--recent paralyses. Br J Oral Maxillofac Surg. 2015;53(10):901-906.

[136] Sforza C, Tarabbia F, Mapelli A, Colombo V, Sidequersky FV, Rabbiosi D, Annoni I, Biglioli F. Facial reanimation with masseteric to facial nerve transfer: a three-dimensional longitudinal quantitative evaluation. J Plast Reconstr Aesthet Surg. 2014;67(10):1378-1386.

[137] Walker DT, Hallam MJ, Ni Mhurchadha S, McCabe P, Nduka C. The psychosocial impact of facial palsy: our experience in one hundred and twenty six patients. Clin Otolaryngol. 2012;37(6):474-477.

[138] Yetiser S, Karapinar U. Hypoglossal-facial nerve anastomosis: a meta-analytic study. Ann Otol Rhinol Laryngol. 2007;116(7):542-549.

[139] Biglioli F, Frigerio A, Colombo V, Colletti G, Rabbiosi D, Mortini P, Dalla Toffola E, Lozza A, Brusati R. Masseteric-facial nerve anastomosis for early facial reanimation. J Craniomaxillofac Surg. 2012;40(2):149-155.

[140] Manktelow RT, Tomat LR, Zuker RM, Chang M. Smile reconstruction in adults with free muscle transfer innervated by the masseter motor nerve: effectiveness and cerebral adaptation. Plast Reconstr Surg. 2006;118(4):885-899.

[141] Smith JW. A new technique of facial reanimation. In: Hueston JH, editor. Transactions of the Fifth International Congress of Plastic Surgery. NSW: Butterworths; 1971.

[142] Martins RS, Socolovsky M, Siqueira MG, Campero A. Hemihypoglossal-facial neurorrhaphy after mastoid dissection of the facial nerve: results in 24 patients and comparison with the classic technique. Neurosurgery. 2008;63(2):310-316.

[143] Hontanilla B, Marré D. Comparison of hemihypoglossal nerve versus masseteric nerve transpositions in the rehabilitation of short-term facial paralysis using the Facial Clima evaluating system. Plast Reconstr Surg. 2012;130(5):662e-672e.

[144] Hontanilla B, Marre D, Cabello A. Facial reanimation with gracilis muscle transfer neurotized to cross-facial nerve graft versus masseteric nerve: a comparative study using the FACIAL CLIMA evaluating system. Plast Reconstr Surg. 2013;131(6):1241-1252.

[145] Banks CA, Bhama PK, Park J, Hadlock CR, Hadlock TA. Clinician-Graded Electronic Facial Paralysis Assessment: The eFACE. Plast Reconstr Surg. 2015;136(2):223e-230e.

[146] Roland JT Jr, Lin K, Klausner LM, Miller PJ. Direct Facial-to-Hypoglossal Neurorrhaphy with Parotid Release. Skull Base. 2006;16(2):101-108.

[147] Sforza C, Guzzo M, Mapelli A, Ibba TM, Scaramellini G, Ferrario VF. Facial mimicry after conservative parotidectomy: a three-dimensional optoelectronic study. Int J Oral Maxillofac Surg. 2012;41(8):986-993.

[148] Gibelli D, De Angelis D, Poppa P, Sforza C, Cattaneo C. An Assessment of How Facial Mimicry Can Change Facial Morphology: Implications for Identification. J Forensic Sci. 2017;62(2):405-410.

[149] Djordjevic J, Jadallah M, Zhurov AI, Toma AM, Richmond S. Three-dimensional analysis of facial shape and symmetry in twins using laser surface scanning. Orthod Craniofac Res. 2013;16(3):146-160.

[150] Popat H, Richmond S, Playle R, Marshall D, Rosin P, Cosker D. Three-dimensional motion analysis - an exploratory study. Part 1: assessment of facial movement. Orthod Craniofac Res. 2008;11(4):216-223.

[151] Popat H, Richmond S, Playle R, Marshall D, Rosin P, Cosker D. Three-dimensional motion analysis - an exploratory study. Part 2: reproducibility of facial movement. Orthod Craniofac Res. 2008;11(4):224-228.

[152] Okada E. Three-dimensional facial simulations and measurements: changes of facial contour and units associated with facial expression. J Craniofac Surg. 2001;12(2):167-174.

[153] Sidequersky FV, Mapelli A, Annoni I, Zago M, De Felício CM, Sforza C. Three-dimensional motion analysis of facial movement during verbal and nonverbal expressions in healthy subjects. Clin Anat. 2016;29(8):991-997.

[154] Sforza C, Frigerio A, Mapelli A, Mandelli F, Sidequersky FV, Colombo V, Ferrario VF, Biglioli F. Facial movement before and after masseteric-facial nerves anastomosis: a three-dimensional optoelectronic pilot study. J Craniomaxillofac Surg. 2012;40(5):473-479.

[155] Sidequersky FV, Verzé L, Mapelli A, Ramieri GA, Sforza C. Quantification of facial movements by optical instruments: surface laser scanning and optoelectronic three-dimensional motion analyzer. J Craniofac Surg. 2014;25(1):e65-70.

[156] https://www.canfieldsci.com/imaging-systems/vectra-h1-3d-imaging-system/ accessed on October 27th 2017.

[157] Camison L, Bykowski M, Lee WW, Carlson JC, Roosenboom J, Goldstein JA, Losee JE, Weinberg SM. Validation of the Vectra H1 portable three-dimensional photogrammetry system for facial imaging. Int J Oral Maxillofac Surg. 2017; Sep 14.

[158] https://www.facebase.org/, accessed on accessed on October 27th 2017.

5. PhD WRITING ACTIVITY

5.1 Abstracts

- Codari M, Caffini M, Baselli G, Tartaglia GM, **Pucciarelli V**, Zago M, Sforza C. Evaluation of different registration approaches in 3D cephalometric landmark estimation. Italian journal of Anatomy and Embryology 2014;119(1);48.
- Codari M, Guidugli GA, Tartaglia GM, **Pucciarelli V**, Pisoni L, Ferrario VF. Morphometric parameters for nasal septum deviation identification in CBCT data. Italian journal of Anatomy and Embryology 2014;119(1);49.
- **Pucciarelli V**, Codari M, Girardi A, Gustinetti C, Tartaglia GM, Caffini M, Baselli G, Sforza C. Evaluation of accuracy and reproducibility in manual point picking during 3D cephalometry on CBCT data. Italian journal of Anatomy and Embryology 2015;120(1);84.
- Dolci C, **Pucciarelli V**, Ferrario VF, Sansone V. 3D facial features in Andersen-Tawil syndrome: a family report. Italian journal of Anatomy and Embryology 2015;120(1);78.
- Dolci C, **Pucciarelli V**, Codari M, Rusconi FME, Marelli S, Trifirò G, Pini A. The face in Marfan Syndrome: a 3D Morphometric Analysis. Italian Journal of Anatomy and Embryology. 2016;121(1);120.

- Pisoni L, Codari M, Galli S, **Pucciarelli V,** Rusconi FME, Tartaglia GM, Dolci C. Comparison of direct linear measurements on dental plaster cast and digital measurements obtained from laser scanner and Con eBeam CT dental models. Italian Journal of Anatomy and Embryology. 2016;121(1);119.
- Codari M, **Pucciarelli V**, Stangoni F, Guidugli GA, Tartaglia GM, Sforza C. Assessment of facial asymmetry using stereophotogrammetry. Italian Journal of Anatomy and Embryology. 2016;121(1);124.
- Baserga C, Segna E, **Pucciarelli V**, Raffaele S, Romano M, Bolzoni A, Muratori S, Cambiaghi S, Sforza C, Giannì AB, Baj A. Efficacy of autologous fat grafting in the treatment of Parry Romberg Syndrome valuated with 3dimensional photogrammetry. 23rd Congress of the European Association For Cranio Maxillo-Facial Surgery.
- Cullati FA, Mapelli A, Romano M, **Pucciarelli V**, Rusconi FME, Sidequersky FV, Giannì AB, Baj A, Sforza C. Soft-tissue morphology and mimicry changes after Bimaxillary Surgery in Class III patients: a longitudinal long term study. 23rd Congress of the European Association For Cranio Maxillo-Facial Surgery.
- **Pucciarelli V**, Gibelli D, Caplova Z, Codari M, Dolci C, Sforza C. Facial and labial movements in different types of smile: quantification through 3D-3D superimposition techniques. 1st IDBN Congress, Bologna, May 25th and 26th 2017.
- Dolci C, **Pucciarelli V**, Ferrario VF, Gibelli D, Marelli S, Trifirò G, Pini A. 3D Morphometric evaluation of the face in Marfan syndrome: a better definition of dysmorphic features. Italian Journal of Anatomy and Embryology. 2017;122(1);83.
- Dolci G, Gibelli D, Borlando A, **Pucciarelli V**, Tartaglia GM, Cattaneo C, Sforza C. How to pinpoint the greater palatine foramen: a metrical analysis applied to a contemporary skeletal collection. Italian Journal of Anatomy and Embryology. 2017;122(1);84.
- Gibelli D, **Pucciarelli V**, Fornarelli G, Loviglio A, Dolci C, Sforza C. A novel approach to the assessment of anatomical uniqueness of ears: application of 3D-3D surface registration. Italian Journal of Anatomy and Embryology. 2017;122(1);101.
- **Pucciarelli V**, Mastella C, Bertoli S, Alberti K, De Amicis R, Battezzati A, Baranello G, Sforza C. 3D stereophotogrammetric facial analysis of SMAII patients. Italian Journal of Anatomy and Embryology. 2017;122(1);174.

- **Pucciarelli V**, Ulaj E, tarabbia F, Gibelli D, Biglioli F, Sforza C. Stereophotogrammetric assessment of the smiling capability after facial reanimation surgery. Italian Journal of Anatomy and Embryology. 2017;122(1);175.
- Segna E, **Pucciarelli V**, Beltramini G, Sforza C, Baj A. Sclérodermies du visage chez les enfants: évaluation de l'efficacité du lipofilling par photo 3D. 53^{éme} Congrès de la Societé Française de stomatologie, chirurgie maxillo-faciale et chirurgie orale, 4-7 Octobre 2017.

5.2 Papers (published)

- Codari M, **Pucciarelli V**, Pisoni L, Sforza C. Laser scanner compared with stereophotogrammetry for measurements of area on nasal plaster casts. British Journal of Oral and Maxillofacial Surgery. 2015;53(8):769-70. **Impact Factor 1.131, 3rd quartile for DENTISTRY, ORAL SURGERY & MEDICINE**. **doi: 10.1016/j.bjoms.2015.05.007.**
- Dolci C, Pucciarelli V, Codari M, Gibelli DM, Marelli S, Trifirò G, Pini A, Sforza C. 3D Craniofacial Morphometric Analysis Of Young Subjects With Marfan Syndrome: A Preliminary Report. Proceedings of the 6th International Conference and Exhibition on 3D body scanning technologies, Lugano, October 2015. **doi: 10.15221/15.054.**
- **Pucciarelli V**, Pisoni L, De Menezes M, Ceron-Zapata AM, Lopez Palacio AM, Codari M, Gibelli DM, Sforza C. Palatal Volume Changes In Unilateral Cleft Lip And Palate Paediatric Patients. Proceedings of the 6th International Conference and Exhibition on 3D body scanning technologies, Lugano, October 2015. **doi: 10.15221/15.139.**
- **Pucciarelli V**, Codari M, Invernizzi C, Bertoli S, Battezzati A, De Amicis R, De Giorgis V, Veggiotti P, Sforza C. Three-Dimensional Craniofacial Features of Glut1 Deficiency Syndrome Patients. Proceedings of the 6th International Conference and Exhibition on 3D body scanning technologies, Lugano, October 2015. **doi: 10.15221/15.061.**
- Codari M, Zago M, Guidugli GA, Pucciarelli V, Tartaglia GM, Ottaviani F, Righini S, Sforza C. The nasal septum deviation index (NSDI) based on CBCT data. Dentomaxillofacial Radiology. 2016;45(2):20150327. **Impact factor 1.919, 2nd quartile for DENTISTRY, ORAL SURGERY & MEDICINE. doi: 10.1259/dmfr.20150327.**
- Sforza C, Dolci C, Gibelli DM, Codari M, **Pucciarelli V**, Ferrario VF, Elamin F. Age-related and sex-related changes in the normal soft tissue profile of native Northern Sudanese subjects: a cross-sectional study. British Journal of Oral and Maxillofacial Surgery. 2016;54(2):192-7.

Impact Factor 1.131, 3rd quartile for DENTISTRY, ORAL SURGERY & MEDICINE. doi: 10.1016/j.bjoms.2015.11.015.

- Codari M, **Pucciarelli V**, Tommasi DG, Sforza C. Validation of a technique for integration of a digital dental model into stereophotogrammetric images of the face using cone-beam computed tomographic data. British Journal of Oral and Maxillofacial Surgery. 2016;54(5):584-6. **Impact factor 1.237, 3rd quartile for DENTISTRY, ORAL SURGERY & MEDICINE. doi: 10.1016/j.bjoms.2016.01.019.**
- Gibelli DM, De Angelis D, Lupi R, Danesino P, Maric M, **Pucciarelli V**, Sforza C. The application of 3D image acquisition systems to palatal rugae: a technical improvement for personal identification. Proceedings of the 7th International Conference and Exhibition on 3D body scanning technologies. **doi: 10.15221/16.105.**
- Dolci C, **Pucciarelli V**, Codari M, Marelli S, Trifirò G, Pini A, Sforza C. 3D Morphometric Evaluation of Craniofacial Features in Adult Subjects With Marfan Syndrome. Proceedings of the 7th International Conference and Exhibition on 3D body scanning technologies. **doi: 10.15221/16.098.**
- **Pucciarelli V**, Gibelli DM, Codari M, Rusconi FME, Cappella A, Cattaneo C, Sforza C. Laser scanner versus stereophotogrammetry: a three-dimensional quantitative approach for morphological analysis of pubic symphysis. Proceedings of the 7th International Conference and Exhibition on 3D body scanning technologies. **doi: 10.15221/16.080.**
- **Pucciarelli V**, Bertoli S, Codari M, Veggiotti P, Battezzati A, Sforza C. Facial Evaluation in Holoprosencephaly. Journal of Craniofacial Surgery. 2017;28(1):e22-e28**. Impact factor 0.7, 4th quartile for SURGERY. doi: 10.1097/SCS.0000000000003171.**
- Codari M, **Pucciarelli V**, Stangoni F, Zago M, Tarabbia F, Biglioli F, Sforza C. Facial thirds-based evaluation of facial asymmetry using stereophotogrammetric devices: Application to facial palsy subjects. Journal of Craniomaxillofacial Surgery. 2017;45(1):76-81. **Impact factor 1.58, 2nd quartile for DENTISTRY, ORAL SURGERY & MEDICINE. doi: 10.1016/j.jcms.2016.11.003.**
- **Pucciarelli V**, Tarabbia F, Codari M, Guidugli GA, Colletti G, Dell'Aversana Orabona G, Bianchi B, Sforza C, Biglioli F. Stereophotogrammetric Evaluation of Labial Symmetry After Surgical Treatment of a Lymphatic Malformation. Journal of Craniofacial Surgery.

2017;28(4):e355-e358. **Impact factor 0.7, 4th quartile for SURGERY. doi: 10.1097/SCS.0000000000003601.**

- **Pucciarelli V**, Bertoli S, Codari M, De Amicis R, De Giorgis V, Battezzati A, Veggiotti P, Sforza C. The face of Glut1-DS patients: A 3D Craniofacial Morphometric Analysis. Clinical Anatomy. 2017;30(5):644-652. **Impact factor 1.82; 2nd quartile for ANATOMY & MORPHOLOGY. doi: 10.1097/SCS.0000000000003601.**
- Segna E, **Pucciarelli V**, Beltramini GA, Sforza C, Silvestre FJ, Giannì AB, Baj A. Parry Romberg Syndrome and linear facial scleroderma: management in pediatric population. Journal of Biological Regulators and Homeostatic Agents. 2017 Apr-Jun;31(2 Suppl 1):131-138. **Impact factor 1.46; 4th quartile for ENDOCRINOLOGY & METABOLISM.**
- Gibelli DM, Borlando A, Dolci C, **Pucciarelli V**, Cattaneo C, Sforza C. Anatomical characteristics of greater palatine foramen: a novel point of view. Surgical and Radiologic Anatomy. 2017 [Epub ahead ofprint]. **Impact factor 1.05, 3rd quartile for ANATOMY & MORPHOLOGY. doi: 10.1007/s00276-017-1899-7.**
- Gibelli DM, **Pucciarelli V**, Pisoni L, Rusconi MEF, Tartaglia GM, Sforza C. Quantification of dental movements in orthodontic follow-up: a novel approach based on registration of 3D models of dental casts. Stomatology Education Journal. 2017;4(1):55-61.
- **Pucciarelli V**, Gibelli D, De Angelis D, Poppa P, Commaudo M, Codari M, Dolci C, Sforza C. Third-based facial similarities and differences of monozygotic twins: a stereophotogrammetric 3D assessment. Proceedings of the 8th International Conference and Exhibition on 3D Body Scanning Technologies, Montreal, QC, Canada, 11-12 Oct, 2017. **doi: 10.15221/17.226.**
- Gibelli D, **Puciarelli V**, codari M, Pisoni L, Dolci C, Sforza C. Mirroring procedures for the assessment of asymmetry of different anatomical structures of the cranium: a protocol based on 3D-3D superimposition. Proceedings of the 8th International Conference and Exhibition on 3D Body Scanning Technologies, Montreal, QC, Canada, 11-12 Oct, 2017. **doi: 10.15221/17.066.**
- **Pucciarelli V**, Piazza E, Ragona F, Gibelli D, Granata T, Dolci C, Sforza C. Three-dimensional stereophotogrammetric analysis of adults affected by Dravet syndrome. Proceedings of the 8th International Conference and Exhibition on 3D Body Scanning Technologies, Montreal, QC, Canada, 11-12 Oct, 2017. **doi: 10.15221/17.163.**

- Sforza C, Ulaj E, Gibelli DM, Allevi F, **Pucciarelli V**, Tarabbia F, Ciprandi D, Dell'Aversana Orabona G, Dolci C, Biglioli F. 3D-3D superimposition methods applied to patients with facial palsy: an innovative method for assessing the success of facial reanimation procedures. British Journal of Oral and Maxillofacial Surgery 2018;56:3-7. **Impact factor 1.21, 3rd quartile for DENTISTRY, ORAL SURGERY & MEDICINE. doi: 10.1016/j.bjoms.2017.11.015.**
- **Pucciarelli V**, Gibelli D, Barni L, Gagliano N, Dolci C, Sforza C. Assessing normal smiling function through 3D-3D surfaces registration: an innovative method for the assessment of facial mimicry. Aesthetic Plastic Surgery 2017; Dec 20 [Epub ahead of print]. **Impact factor 1.32, 2nd quartile for MEDICINE & SURGERY. doi: 10.1007/s00266-017-1028-3.**
- Gibelli DM, De Angelis D, **Pucciarelli V**, Riboli F, Ferrario VF, Dolci C, Sforza C, Cattaneo C. Application of 3D models of palatal rugae to personal identification: hints at identification from 3D-3D superimposition techniques. International Journal of Legal Medicine 2017; Nov 20 [Epub ahead of print]. **Impact factor 2.38, 1st quartile for MEDICINE PATHOLOGY AND FORENSIC MEDICINE. doi: 10.1007/s00414-017-1744-x.**
- Gibelli DM, **Pucciarelli V**, Poppa P, De Angelis D, Cummaudo M, Pisoni L, Codari M, Cattaneo C, Sforza C. 3D-3D facial superimposition between homozygotic twins: a novel morphological approach to the assessment of differences due to environmental factors. Legal Medicine 2017;31:33-37. **Impact factor 1.27, 2nd quartile for PATHOLOGY AND FORENSIC MEDICINE. doi: 10.1016/j.legalmed.2017.12.011.**
- Biglioli F, Zago M, Allevi F, Ciprandi D, Dell'Aversana Orabona G, **Pucciarelli V**, Rabbiosi D, Pacifici I, Tarabbia F, Sforza C. Reanimation of the paralyzed lids by cross-face nerve graft and platysma transfer. British Journal of Oral and Maxillofacial Surgery. In press. **Impact Factor 1.131, 3rd quartile for DENTISTRY, ORAL SURGERY & MEDICINE**. **doi: 10.1016/j.jcms.2017.12.022.**

5.2.1 Papers (Accepted)

- Gibelli DM, **Pucciarelli V**, Ferrario VF, Dolci C, Sforza C. Anatomic uniqueness of ear morphology. Plastic and Reconstructive Surgery. Accepted September 2017. **Impact factor 3.84, 1st quartile for SURGERY.**

- Dolci C, Pucciarelli V, Gibelli DM, Codari M, Marelli S, Trifirò G, Pini A, Sforza C. The face in Marfan syndrome: a 3D quantitative approach for a better definition of dysmorphic features. Clinical Anatomy. Accepted December 2017. **Impact factor 1.82; 2nd quartile for ANATOMY & MORPHOLOGY.**

5.3 Papers (Submitted)

- Gibelli DM, Codari M, **Pucciarelli V**, Dolci C; Sforza C. How lips are modified by facial expressions: a quantitative assessment through 3D-3D superimposition. Submitted to Journal of Oral and Maxillofacial Surgery on September 2017.
- Gibelli DM, Cellina M, Gibelli S, Oliva AG, Termine G, **Pucciarelli V**, Dolci C, Sforza C. Assessing symmetry of zygomatic bone through 3D segmentation on CT scans and "mirroring" procedure: a contribution for reconstructive maxillofacial surgery. Submitted to Journal of Cranio maxillo-facial Surgery on September 2017.
- Gibelli DM, De Angelis D, **Pucciarelli V**, Dolci C, Sforza C. Quantification of odontological differences of the upper first molar through 3D-3D superimposition: a novel method for assessing anatomical uniqueness. Submitted to Journal of Forensic Science on September 2017.
- Gibelli D, **Pucciarelli V**, Cappella A, Dolci C, Sforza C. Are portable stereophotogrammetric devices reliable in facial imaging? A validation study of Vectra H1 device. Submitted to Journal of Oral and Maxillofacial Surgery on December 2017.
- **Pucciarelli V**, Baserga C, Codari M, Beltramini GA, Sforza C, Giannì AB. Three-dimensional stereophotogrammetric evaluation of the efficacy of autologous fat grafting in the treatment of Parry Romberg Syndrome. Submitted to Journal of Craniofacial Surgery on December 2017.

6. COURSES, SEMINARS AND EXAMS

- "Anthropology" (Professor Cristina Cattaneo) 6 CFU, 48 hours.
- "Giornata di Studio dedicate alle biotecnologie" Premio Sapio (October 21, 2015).
- "Awarding with Medical Honorary Degree of Stephen Coplan Harrison (December 10, 2015).
- "How to write a Grant" (Seminario Bando Telethon) (December 12, 2015).

- “Lezioni di futuro” (Bioetics seminar) (January 28, 2016).
- “Stem Girls, le carriere del futuro” (April 7, 2016).
- “Il farmaco per la qualità della vita: sinergie tra accademia e impresa, realtà e prospettive occupazionali”. (May 19, 2016).
- “Il futuro nelle biotecnologie: opportunità d’innovazione e crescita sostenibile” (May 20, 2016). “Darwin medico” (May 20, 2016).
- “Il volto, la chirurgia e le tecnologie 3D. Successi e frontiere maxillo-facciali” (May 20, 2016). “Insegnamenti dallo studio delle malattie rare” (May 21, 2016).
- “Statistics” (May 8, 2015). Rating: 30/30 cum Laude. (Professor Alberto Porta), 3 CFU, 24 hours.
- “Anatomy of the Head and Neck” (February 2015). (Professor Chiarella Sforza) 2 CFU, 16 hours.
- “Bilancio e sviluppo delle competenze per il lavoro” (July 2017, COSP UNIMI).

6.1 Conferences

- 6th International Conference and Exhibition on 3D Body Scanning technologies, Lugano, Switzerland, October 27-28, 2015.
- 7th International Conference and Exhibition on 3D Body Scanning technologies, Lugano, Switzerland, November 30-December 1, 2016.
- 1st European Conference on Glut1 Deficiency syndrome. Milan, October 7-8, 2016.
- “Sindrome di Dravet, Attualità terapeutiche e Cliniche”, Pavia October 19, 2016.
- I Congresso IDBN, Bologna, May 25-26, 2017.
- 71° Congresso della Società Italiana di Anatomia e Istologia, Taormina, September 20-22, 2017.
- 8th International Conference and Exhibition on 3D Body Scanning Technologies, Montreal, QC, Canada, October 11-12, 2017.

7. TEACHING ACTIVITIES

- Elective course of 3D and functional anatomy of the maxillofacial district (May 26-27, 2015, for Medicine and Dentistry Students).

- Elective course of anatomy (June 24, 2015, for nursing and obstetrics students).
- Elective course of 3D and functional anatomy of the maxillofacial district (May 31- June 1, 2016, for Medicine and Dentistry Students).
- Elective course of anatomy (June 17, 2016 for nursing and obstetrics students).
- Elective course of 3D and functional anatomy of the maxillofacial district (May 30- 31, 2017, for Medicine and Dentistry Students).
- Tutor, high school students attending the Università degli Studi di Milano, Department of Biomedical Science for Health, Laboratory of Functional Anatomy of the Stomatognatic Apparatus (Minister project "Alternanza Scuola Lavoro").
- Tutor of several master thesis students (medicine and dentistry).
- Winner of an assignment of tutoring and integrative teaching activity for the Human Anatomy course, MD course, Università degli Studi di Milano.

8. GRANTS

- Participation to the project: "3D dental and soft-tissue facial modifications in adults treated with invisible dental aligners". PI Prof.ssa Chiarella Sforza, 3D Objects and data software 2017.

9. REVIEWER ACTIVITY

- Arab Journal of Forensic Sciences & Forensic Medicine
- Journal of Esthetic and Restorative Dentistry
- Journal of Oral health and Craniofacial Sciences